

Formation, evolution, and inversion of the middle Tertiary Diligencia basin, Orocochia Mountains, southern California

Richard D. Law*
Kenneth Eriksson
Cole Davisson

Department of Geological Sciences, Virginia Polytechnic Institute and State University, Blacksburg, Virginia 24061-0420, USA

ABSTRACT

The Diligencia basin, located in the eastern Orocochia Mountains of southern California, contains 1500–2000 m of Oligocene–Miocene continental, siliciclastic sedimentary rocks and subordinate limestone and evaporite deposits, intercalated with basaltic lavas. These rocks are locally intensely folded and faulted, defining in present-day coordinates an elongate east-west-trending basin, and are unconformably overlain by flat-lying late Pliocene(?) and Pleistocene alluvial deposits. The sedimentological, stratigraphic, and structural history of the basin is compatible with late Oligocene–early Miocene formation as a half-graben basin produced by orthogonal, Basin and Range-type extension, and latest Miocene to Pliocene basin inversion in either a localized transpressional Transverse Range regime, or a more diffuse compressional regime associated with north-south shortening of the entire Mojave block.

Facies associations in the lower part of the Diligencia basin display a distinctly asymmetric distribution across the basin, indicating deposition in a half-graben with a steep, possibly fault controlled, south-facing northern escarpment and a more gentle north-facing southern slope. Paleocurrent data, particularly from high-energy deposits on the northern basin margin, indicate stream flow toward the southeast to south-southeast, oblique to the deformed basin margins, and suggest an approximate northeast to east-northeast strike for the basin before deformation. Previously published paleomagnetic data, however, indicate that the elongate, currently east-

west-trending, fault block containing the Diligencia basin has rotated clockwise by as much as 110° about a vertical axis (angle depends on data and model used) since deposition ceased. If correct, this would suggest that the basin may have originally opened to between the northeast and east-northeast, subparallel to well-documented extension directions in Miocene age basins in the Mojave Desert to the east. Clockwise rotation on east-west fault blocks exposed in this region has previously been bracketed as between ca. 10 and 4.5 Ma. Structural and paleomagnetic data indicate that inversion of the Diligencia basin occurred after block rotation, implying a latest Miocene to Pliocene age for inversion. We speculate that basin inversion within a north-south (and still active) compressive stress field resulted from the locking, and subsequent internal deformation, of this previously passively rotating elongate crustal block.

Keywords: basin (structural), Basin and Range province, grabens, Mojave Desert, tectonic models, Transverse Ranges.

INTRODUCTION

The late Oligocene–Miocene stratigraphic record of western California is characterized by a series of areally restricted, but thick, non-marine sedimentary successions (Fig. 1) (Blake et al., 1978; Crowell, 1987, 1993a). The basins that host these successions developed during the transition from a convergent to a transform plate margin (Atwater, 1970; Blake et al., 1978; Graham et al., 1984; Crowell, 1987; Nicholson et al., 1994; Bohannon and Parsons, 1995; Dickinson, 1997; Atwater and Stock, 1998). Formation of some of the younger basins, such as the Ridge basin, which began forming in late middle Miocene

time (ca. 12 Ma), was clearly controlled by strike-slip tectonics (Crowell and Link, 1982). However, the role that strike-slip motion may have played in development of many of the older basins, particularly those that developed during late Oligocene to early Miocene time in southern California, during the transition from regional-scale extensional to strike-slip tectonics, is less clear (cf. Richard, 1988; Tennyson, 1989; Weldon et al., 1993). For example, whereas in central California, formation of the La Honda (Stanley, 1985, 1987) and Cuyama (Bartow, 1990, but also see Buckner et al., 1991) basins during early Miocene time may have been controlled by strike-slip deformation, in southern California formation of similar age basins such as the Plush Ranch (Cole and Stanley, 1995), southern San Joaquin (DeCelles, 1988; Goodman and Malin, 1992), and Soledad (Hendrix and Ingersoll, 1987; Hendrix, 1993) basins appears to be related to extensional faulting.

The Diligencia basin, located in the Orocochia Mountains of southern California (Fig. 1), is the most southerly of these basins and has also been interpreted as being extensional in origin (e.g., Spittler and Arthur, 1982). As much as 2000 m of uppermost Oligocene and lower Miocene irregularly interbedded non-marine conglomerate, sandstone, siltstone, limestone, and associated volcanic flows and intrusions are preserved in this currently east-west-trending elongate basin. These rocks, which are referred to as the Diligencia Formation (Crowell, 1960, 1962, 1975; Spittler and Arthur, 1982; Crowell, 1993b), are considered to have filled an east-west-trending intermontane basin (Crowell, 1975) in the form of a graben (Bohannon, 1975), or an asymmetric half-graben with either a steep northern flank (Spittler and Arthur, 1982) or a steep southern flank (Robinson and Frost, 1989, 1991, 1996) in present-day coordinates.

*E-mail: rdlaw@vt.edu.

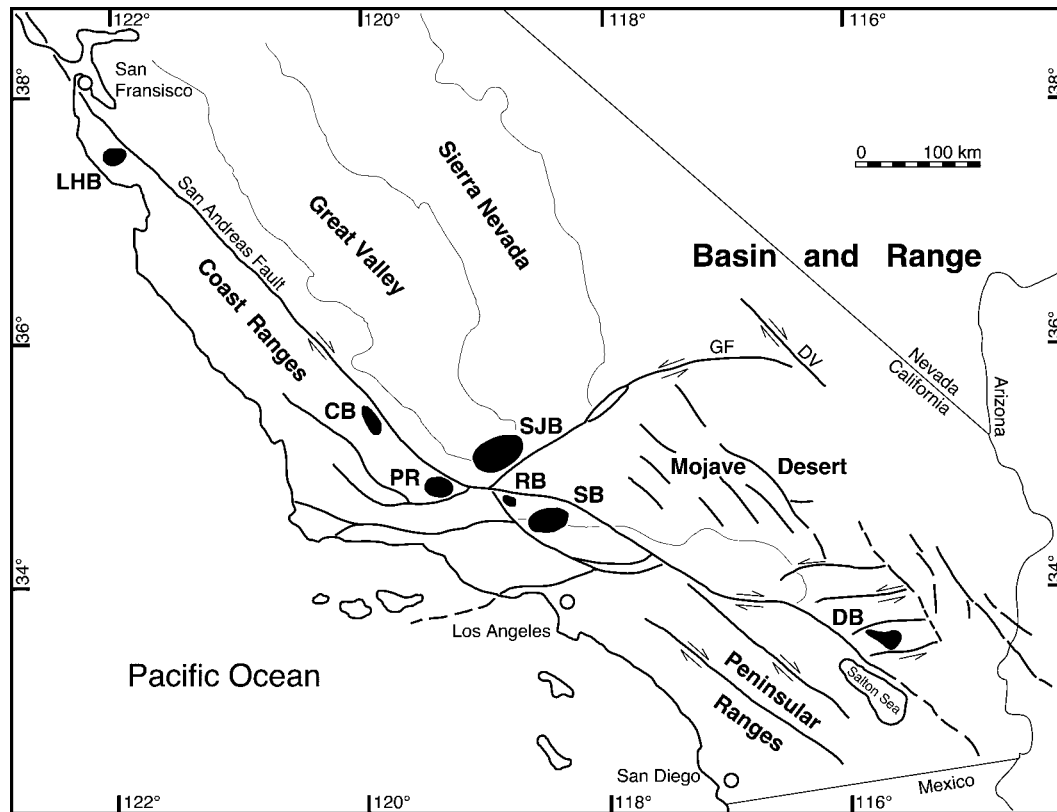


Figure 1. The San Andreas fault system and selected late Oligocene–Miocene basins in central and southern California. CB—Cuyama basin; DB—Diligencia basin; DV—Death Valley fault zone; GF—Garlock fault; LHB—La Honda basin; PR—Plush Ranch basin; RB—Ridge basin; SB—Soledad basin; SJB—Southern San Joaquin basin.

In this paper we present a stratigraphic and sedimentologic analysis of the lower Diligencia Formation and an analysis of the postdepositional tectonic structures in the basin. The sedimentological, stratigraphic, and structural history of the basin is compatible with late Oligocene–early Miocene formation as a half-graben produced by orthogonal, Basin and Range–type extension, and latest Miocene to Pliocene basin inversion in either a localized transpressional Transverse Range regime, or a more diffuse contractional regime associated with north-south shortening of the entire Mojave block. Clockwise block rotation of no more than 110° followed basin infilling but preceded inversion. Formation and inversion of the Diligencia basin are thus direct consequences of the changing tectonic regime in southern California during late Tertiary time.

TECTONIC FRAMEWORK

The Neogene evolution of southern California has been controlled by the development of two contrasting tectonic provinces. Deformation to the east of the study area was dom-

inated by extensional faulting within the Basin and Range province, whereas structural evolution of the coastal region to the west is traditionally thought to have been controlled by strike-slip faulting on the San Andreas fault system. The Diligencia basin is located in the approximate border zone between these provinces (Figs. 1 and 2).

East of the Diligencia basin, in the Mojave Desert and lower Colorado River areas of the Basin and Range province, late Oligocene–early Miocene faulting was followed by a major episode of low-angle extensional deformation and tilting after 22 Ma (Sherrod and Tosdal, 1991). Extension was oriented northeast-southwest ($N50^\circ\text{--}60^\circ\text{E}$) (Glazner and Bartley, 1984; Wust, 1986; Best, 1988; Bartley and Glazner, 1991; Dokka and Ross, 1995), and horizontal extensions of 10%–20% are indicated by the angular relationships between tilted strata and the underlying faults (Sherrod and Tosdal, 1991). Extension ceased by 20 Ma in some parts of the region, after which fluvial-lacustrine systems filled many grabens and half-grabens (Simpson et al., 1991). A synthesis of available age data for timing of extension and volcanism in the Ba-

sin and Range province was done by Stewart (1998); available data from the Colorado River region east of the Diligencia basin indicate an age of 21–16 Ma for extensional faulting and tilting of strata. The timing for cessation of Miocene extension is generally poorly known, however (Sherrod and Tosdal, 1991), and extension may have progressively waned from 19 to 15 Ma (Tennyson, 1989). Bartley et al. (1990) argued that following extension, the Mojave block was locally subjected to folding and thrust faulting associated with north-south contraction in late Cenozoic time. This contraction may have begun as early as 19 Ma in the Cady and Newberry Mountains (Fig. 2), and could be continuing at the present time (Bartley et al., 1990).

In southern California, the San Andreas fault system consists of a network of northwest-striking dextral strike-slip faults, and east- to northeast-striking sinistral strike-slip faults (Fig. 2). The northwest- and east- to northeast-trending faults are present both to the southwest of the modern San Andreas fault zone and northeast of the fault zone in the Mojave Desert section of the Basin and Range province. The Transverse Ranges comprise east-west-trending structural

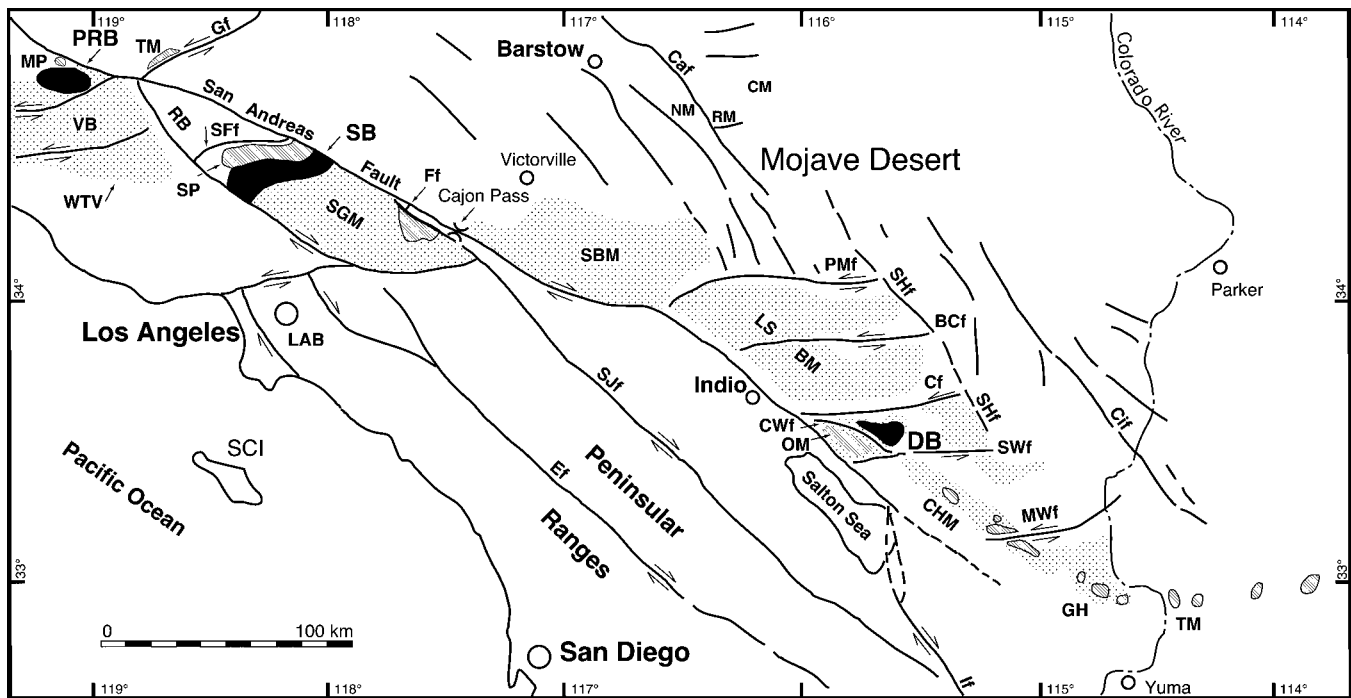


Figure 2. Geologic map of southern California showing locations of selected faults and Neogene basins referred to in text. The Diligencia (DB), Soledad (SB), and Plush Ranch (PRB) basins are indicated by black ornament; exposures of Rand-Pelona-Orocopia Schists are indicated by diagonal rules. Western Transverse Ranges, San Gabriel, San Bernardino, Little San Bernardino, and Chocolate Mountains are indicated by stipple. BCf—Blue Cut fault; Caf—Calico fault; Cf—Chiriaco fault; Cif—Cibola fault; CHM—Chocolate Mountains; CM—Cady Mountains; CWF—Clemens Well fault; Ef—Elsinore fault; Ff—Fenner fault; Gf—Garlock fault; GH—Gavilan Hills; LAB—Los Angeles basin; LSBM—Little San Bernardino Mountains; MP—Mount Pinos; MWf—Mammoth Wash fault; NM—Newberry Mountains; OM—Orocopia Mountains; PMf—Pinto Mountain fault; RM—Rodman Mountains; RB—Ridge basin; SBM—San Bernardino Mountains; SCI—Santa Catalina Island; SFf—San Francisquito fault; SGM—San Gabriel Mountains; SHf—Sheep Hole fault; Sjf—San Jacinto fault; SP—Sierra Pelona; SWf—Salton Wash fault; THM—Tehacapi Mountains; TM—Trigo Mountains; VB—Ventura basin; WTV—western Transverse Ranges. Rand Schist crops out in Tehacapi Mountains; Pelona schist crops out in Mount Pinos, Sierra Pelona, and San Gabriel Mountains; Orocopia Schist crops out in Orocopia, Chocolate, and Trigo Mountains and Gavilan Hills. Mountain ranges located on the eastern side of the San Andreas fault (San Bernardino, Little San Bernardino, and Chocolate Mountains) are referred to as the eastern Transverse Ranges. West-east-trending ranges located to the west of the San Andreas fault are referred to as the western Transverse Ranges; San Gabriel Mountains are referred to as the central Transverse Ranges by some. Adapted from Jacobson (1990), Dillon and Ehlig (1993), Matti and Morton (1993), and Richard (1993).

provinces that crosscut the northwest-southeast-trending structural grain in southern California, and are bordered on the north and south by east-west-trending sinistral strike-slip faults. The northwest-striking faults in the Coastal Ranges and Peninsula Ranges terminate against these east-west faults, although the western Transverse Ranges are dextrally offset from the central and eastern Transverse Ranges by the northwest-striking San Gabriel and San Andreas faults. Within the Mojave Desert region, the east-west-striking sinistral faults are bounded to the east by a zone of northwest-striking dextral strike-slip faults (the Mojave Desert dextral domain of Powell, 1993, p. 63) and to the west by the San Andreas fault system (Fig. 2). Available evidence suggests that movement on all three sets of faults is broadly coeval (Powell, 1993;

Dickinson, 1996), and that distributed dextral and sinistral shear on the northwest- and east-striking faults, respectively, may have resulted in a net dextral shear across the Mojave Desert region (referred to as the Eastern California shear zone by Dokka and Travis, 1990a) of ~50–100 km since late Miocene time (Carter et al., 1987; Dokka and Travis, 1990a, 1990b). Movement on the Eastern California shear zone occurred mainly between 10 and 6 Ma (Dokka et al., 1991, 1998). Distributed dextral and sinistral strike-slip faulting is predicted to have led to significant rotation about vertical axes of the individual crustal blocks between these faults (see reviews by Richard, 1993; Dickinson, 1996). This prediction is strongly supported by paleomagnetic declination data from Neogene volcanic rocks in both the Transverse Ranges

and the Mojave Desert region to the east (Luyendyk et al., 1980, 1985; Hornafius et al., 1986; Carter et al., 1987; Luyendyk, 1991).

Where post-Cretaceous extensional deformation has been recognized in coastal southern California, west of the principal strand of the San Andreas fault system, it has generally been attributed to strike-slip motion (e.g., Wilcox et al., 1973; Crowell, 1974a). However, refinement of calculated Cenozoic plate margin configurations (e.g., Nicholson et al., 1994; Bohannon and Parsons, 1995; Atwater and Stock, 1998) and reevaluation of structural features observed both in outcrop and on seismic reflection profiles (e.g., Wallace, 1982; Engel and Schultejan, 1984; Schultejan, 1984; Legg, 1991; Baker et al., 1991; Fattahipour and Frost, 1991, 1996; Robinson

and Frost, 1991; Pridmore and Frost, 1992; Crouch and Suppe, 1993; Axen and Fletcher, 1998; Bohannon and Geist, 1998) indicate a distinct episode of Miocene extension in coastal southern California of similar age and orientation to the more widely recognized extension in the adjacent Basin and Range province to the east.

Tennyson (1989) argued that there is no evidence for major strike-slip faulting in central and southern California during late Oligocene–early Miocene time (i.e., before 19–18 Ma), and that the transform boundary between the North American and Pacific plates did not form until late-early Miocene time, during the waning stages of Miocene crustal extension. Tennyson (1989) further argued that because basin fills in the Transverse Ranges are the same age as extensional basins in the adjacent Basin and Range province, they may also be extensional in origin, rather than being related to strike-slip faulting.

In central California, the San Andreas fault is generally considered to have become active between 20 and 17 Ma (O'Day and Simms, 1986; Graham et al., 1989; Powell and Weldon, 1992; Atwater and Stock, 1998). In contrast, major strike-slip displacement in southern California on the San Andreas fault system did not begin until about 12 Ma, although some precursor displacement may already have been under way (Crowell, 1993a). Major dextral slip and development of the present-day course of the San Andreas in southern California is primarily a Pliocene and Quaternary event, and the modern active strand of the San Andreas fault from the central Transverse Ranges southward within the Salton Trough (Fig. 2) is probably no older than 5 Ma (Crowell, 1982).

Total dextral slip on the San Andreas fault in central California (north of the junction between the San Gabriel and San Andreas faults) is estimated as 315 ± 10 km, whereas in southern California total displacement on the San Andreas fault may only be 150–160 km (see reviews by Powell and Weldon, 1992; Dillon and Ehlig, 1993; Powell, 1993; Weldon et al., 1993). In order to explain the differences in timing and total slip on the San Andreas fault in central and southern California, a number of tectonic models have been proposed for precursor faulting in southern California. This faulting may have been contemporaneous with early strike-slip motion on the San Andreas in central California, and these early through-going faults were later crosscut and displaced by the modern San Andreas fault. Powell (1981) proposed that one candidate for a precursor fault to the San Andreas

in southern California may be marked by the Clemens Well, Fenner, and San Francisquito faults (Fig. 2). Palinspastic restoration models, based on temporal and lithologic correlation, indicate that the now widely separated latest Oligocene–Miocene Diligencia, Soledad, and Plush Ranch basins (Fig. 2) may have been contiguous before motion on the San Andreas and precursor Clemens Well, Fenner, and San Francisquito fault systems (Crowell, 1962, 1975; Crowell and Walker, 1962; Bohannon, 1975; Powell, 1981, 1993; Matti and Morton, 1993). The various palinspastic restoration models proposed for these Miocene basins were summarized by Frizzell and Weigand (1993).

LOCAL GEOLOGIC SETTING

The Orocochia Mountains are located in the northeastern corner of the Salton Trough on the eastern margin of the Transverse Ranges physiographic province, and near the western edge of the southern Basin and Range province (Figs. 1 and 2). The eastern portion of the Orocochia Mountains comprises the Diligencia basin complex, which includes Oligocene–Miocene sedimentary rocks of the Diligencia Formation (Crowell, 1975), the underlying Eocene Maniobra Formation (Crowell and Susuki, 1959; Johnston, 1961), and associated Proterozoic and Mesozoic crystalline basement terranes (Crowell, 1962; Crowell and Walker, 1962; Robinson and Frost, 1996). A detailed geologic map of the Diligencia basin, together with a series of cross sections drawn at right angles to the basin long axis, was originally presented by Arthur (1974) and Spittler (1974). This map was subsequently published by Spittler and Arthur (1982), and is reproduced in a simplified format in Figure 3, where it is integrated with other previously published studies of the surrounding basement rocks. A representative cross section through the basin is given in Figure 4.

In the following sections describing the sedimentology and structure of the Diligencia basin we use present-day geographic coordinates. However, many crustal blocks in the Transverse Ranges and adjacent Mojave Desert (including the Orocochia Mountains) underwent significant clockwise rotation about vertical axes in late Miocene–Pliocene time (ca. 12–4.3 Ma; Luyendyk et al., 1980, 1985; Carter et al., 1987; Luyendyk, 1991; Richard, 1993; Dickinson, 1996), and present-day compass directions given for prerotation features may not necessarily indicate their original orientation.

Rocks of the Diligencia Formation were briefly described by Crowell (1960, 1962) and are preserved in a currently east-west–trending elongate basin (Fig. 3). The unit was formally named, and a type section designated, by Crowell (1975). The most complete descriptions of the Diligencia Formation are by Arthur (1974), Spittler (1974), and Spittler and Arthur (1982), although Squires and Advocate (1982) described in detail the lower part of the formation in the southeast corner of the basin. The Diligencia Formation consists of a nonmarine siliciclastic succession; basaltic lavas and slightly younger andesitic intrusions in the middle part of the succession are dated as between 23.6 and 21.3 Ma (K-Ar; see Frizzell and Weigand, 1993, and their review of previous age determinations by Crowell, 1973, and Spittler, 1974). Late Arikareean (20–23 Ma; Tedford et al., 1987) or less possibly early Hemingfordian age vertebrate remains were described by Woodburne and Whistler (1973) from the middle part of the succession, ~10 m above the volcanic flows (Nilsen, 1982; Spittler and Arthur, 1982). Because the volcanic rocks come from the middle part of the Diligencia Formation (~700 m above the base of the formation), it is possible that the lowest part of the Diligencia Formation may include Oligocene beds (Crowell, 1993b). No precise upper age limit can be assigned to the formation because of the lack of diagnostic fossils or fresh volcanic rocks in the upper part of the section (Spittler and Arthur, 1982).

The rocks of the Diligencia Formation are deformed into a series of upright kilometer-scale east-west– to northwest-southeast–trending folds that are crosscut by northwest- and northeast-striking faults (Figs. 3 and 4). Hinge lines of the folds are offset by the largest of the northeast-striking faults by as much as 1 km with dominantly sinistral slip (Crowell, 1975). On the north side of the basin the Diligencia Formation unconformably overlies strata of the marine Eocene Maniobra Formation (Crowell and Susuki, 1959), whereas on the southeast side of the basin the formation nonconformably overlies crystalline basement of Proterozoic age (Fig. 3). Here the unconformity is vertical to locally overturned, and laterally passes eastward into a steeply dipping reverse fault (Spittler and Arthur, 1982; Crowell, 1993b). On the southwest side of the basin, rocks of the Diligencia Formation are truncated by the Clemens Well fault (Fig. 3). On the east and northeast sides of the basin the folded and faulted rocks of the Diligencia Formation are overlapped by flat-lying Pliocene(?) and early Pleistocene terrace gravels (Jennings, 1967; Spittler and Arthur, 1982).

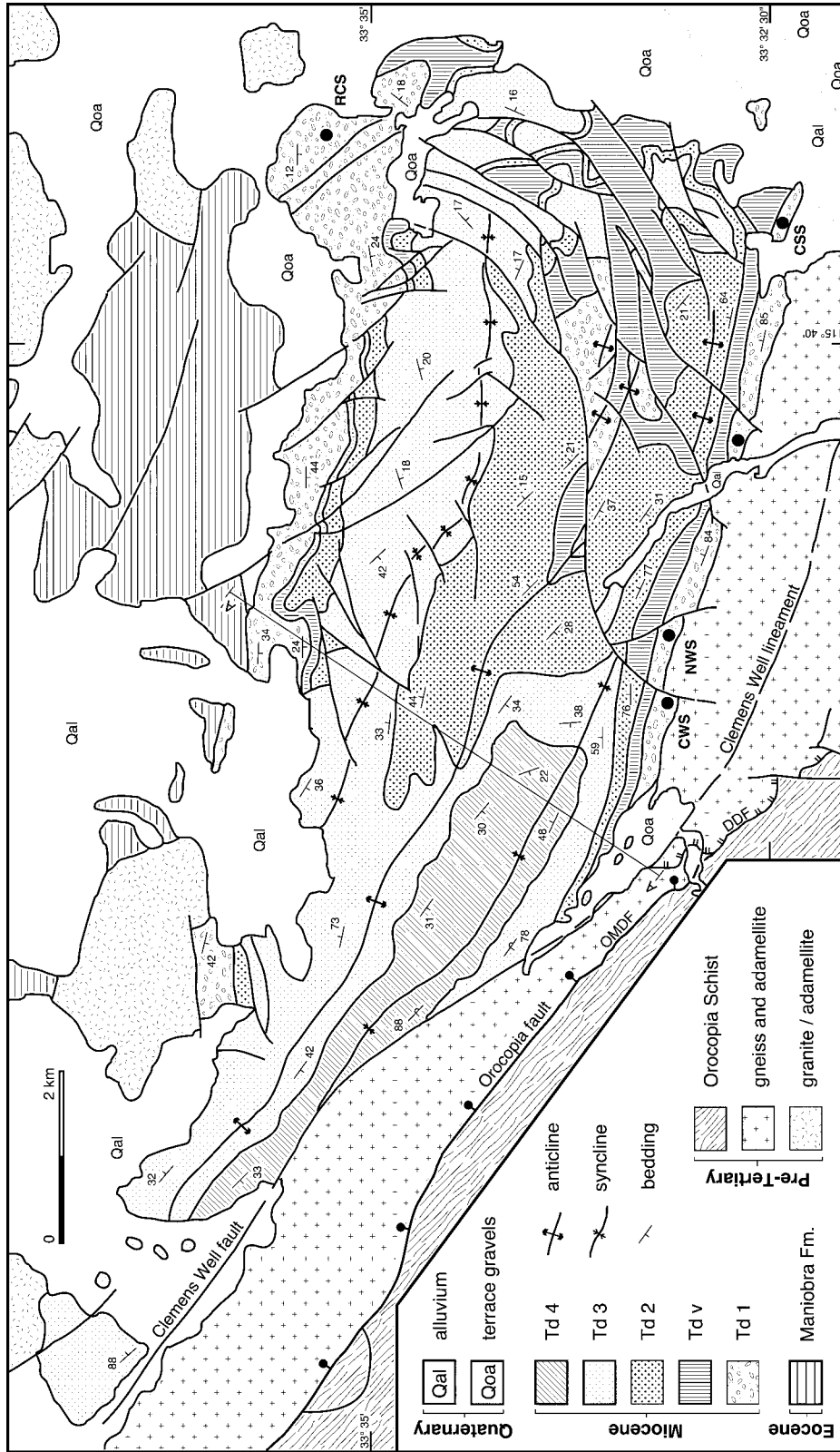


Figure 3. Geologic map of the Diligencia basin, adapted from Crowell and Walker (1962), Jennings (1967), Arthur (1974), Spittler and Arthur (1982), Davison (1993), and Robinson and Frost (1996). Line of cross section (A-A') in Figure 4 and locations of measured stratigraphic sections (Fig. 5) are indicated; CWS—Clemens Well Saddle section; NWS—Name Wall section; BPS—Bullet Peak section; CSS—Canyon Spring section; RCS—Red Canyon section. OMDF—Orocopia Mountains detachment fault (Robinson and Frost, 1996); ball and tick symbol is on downthrown hanging wall; fault was also referred to as the Orocopia fault by Jacobson and Dawson (1995) and the Orocopia thrust by Crowell (1962). DDF—Diligencia detachment fault (Robinson and Frost, 1996); double tick mark is on downthrown hanging wall.

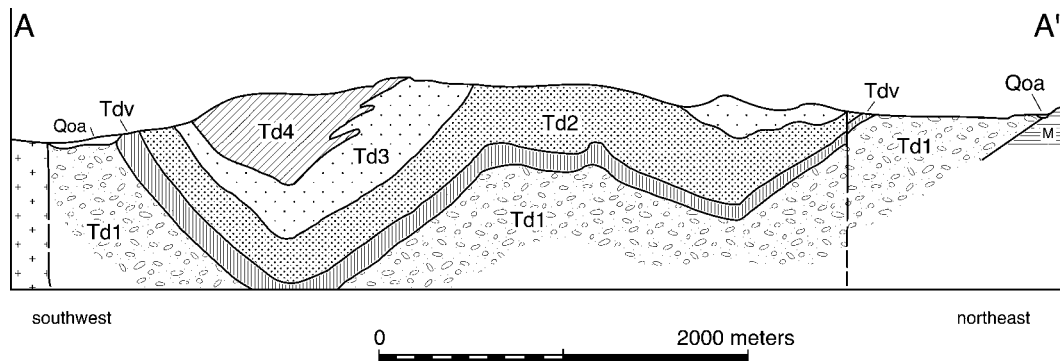


Figure 4. Cross section along line A–A' in Figure 3; adapted from Arthur (1974); for explanation of symbols used see Figure 3.

STRATIGRAPHY AND SEDIMENTOLOGY

The Diligencia Formation is at least 1500 m thick, may locally be as much as 2000 m thick (Spittler and Arthur, 1982), and has been subdivided into four interfingering lithostratigraphic units (Td1–Td4; Spittler and Arthur, 1982). The map distribution of these units is indicated in Figure 3. Unit 1 consists primarily of coarse-grained, alluvial siliciclastic sedimentary rocks that were derived from both the north and south. On the north side of the basin, the basal conglomerate consists primarily of clasts derived from granitic terranes that crop out farther to the north; there is only a minor contribution from the underlying Eocene beds (Spittler and Arthur, 1982; Crowell, 1993b). In contrast, on the south side of the basin, clasts consist mainly of augen gneiss derived from the underlying metamorphic rocks (Spittler and Arthur, 1982; Crowell, 1993b). Unit 1 fines upward into a lacustrine interval of varicolored siltstone, mudstone, and minor limestone and sulfate evaporite. On the southwest side of the basin, conglomerate lenses within the middle and lower upper parts of unit 1 contain clasts of anorthosite, syenite, and granodiorite that were apparently derived from a terrane similar to that preserved in the adjacent hanging wall of the Orocopia fault southwest of the Clemens Well fault (Crowell, 1975) (Fig. 3). No debris from the Orocopia Schist (Fig. 3), however, has yet been recognized within the Diligencia Formation (Crowell, 1993b).

Unit 1 is capped by an interval of basaltic lava flows (Tdv) and intercalated siltstones that are intruded by andesitic sills, dikes, and irregular bulbous intrusions, which suggest emplacement into soft sediments (Crowell, 1993b). Overlying sedimentary rocks of unit 2 comprise mainly varicolored and mottled siltstone, mudstone, and fine-grained sandstone of lacustrine and lake margin origin. Pa-

leocurrent data indicate derivation from the north. Unit 3 consists of multistory successions of conglomerate-breccia, sandstone, siltstone, and mudstone commonly displaying upward-fining patterns. Conglomerate and breccia are confined to the northern outcrop belt and locally directly overlie basement. Monolithologic breccia displaying fitted fabrics probably represents debris flow or, more likely, landslide deposits (Crowell, 1993b). Internal architecture of sediment bodies and aerial distribution of facies, coupled with paleocurrent data, suggest that unit 3 developed as a series of coalescing alluvial fans along the northern basin margin, which passed southward into a flood plain. Vertical transition from unit 2 to 3 indicates that the alluvial system initially built into a playa lake before overrunning the lake as sediment flux increased. Unit 4 is comparable in character to unit 2 and is interpreted as a flood-plain–lake deposit (Spittler and Arthur, 1982). This study focuses on the lower Diligencia Formation (unit 1) because: (1) it provides an opportunity to investigate relationships between basement faulting and sedimentation, and (2) basin inversion structures are most clearly developed adjacent to the basement-cover contact on the southern basin margin.

Methods

Five sections were measured through the lower Diligencia Formation, four along the southern basin margin and one on the northern margin (Fig. 5). The location of each section within the basin is indicated in Figure 3. Where possible, each section was measured in a location where the Diligencia Formation overlies older rocks. Underlying rocks include pre-Tertiary crystalline basement and the Eocene Maniobra Formation. Where exposure permitted, sections were measured up to the first basalt >30 cm thick. The lower Diligen-

cia Formation, as defined here, varies in thickness between 120 and 400 m.

Facies Analysis

Facies identified in the five measured sections can be grouped into three grain-size assemblages: breccia-conglomerate (1); sandstone (2); and siltstone-claystone (3). In addition, a carbonate facies is also distinguished. Two facies associations (1a and 1b) are recognized within the breccia-conglomerate assemblage, whereas the sandstone assemblage consists of four facies associations (2a–2d). The temporal relationships of the facies associations are shown in Figure 5 (A–E). Table 1 summarizes the descriptive characteristics of the facies associations, including paleocurrents. All paleocurrent data are shown on rose diagrams (Fig. 6). Process and paleoenvironmental interpretations of the facies associations are given in Table 2.

BASIN RECONSTRUCTION

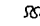

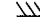
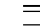
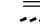

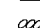



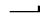
Depositional Systems and their Areal Distribution

Facies associations in the lower Diligencia Formation display a strongly asymmetric distribution across the basin. The present northern margin is characterized by thick and coarse-grained deposits (facies associations 1a, 2a; Fig. 5A), whereas thinner and finer grained deposits are preserved along the present southern basin margin (facies associations 1b, 2b–2d; Fig. 5B).

Facies associations documented from the northern margin of the Diligencia basin (1a and 2a) are interpreted to have been deposited in a very high energy, braided-fluvial system. The remarkably large clast sizes observed in conglomerates (Fig. 7A), as well as the relatively large clast sizes in the conglomeratic sandstone beds (Fig. 7B), indicate that the

Clemens Well Saddle Section

Symbols

-  convoluted bedding
-  ripple marks
-  tabular cross-beds
-  planar stratification
-  planar lamination
-  mudstone rip-ups
-  fining-upwards interval
-  imbricated clasts
-  current lineations
-  desiccation cracks
-  fault in section

Lithology

-  mudstone
-  sandy limestone
-  sandstone
-  trough cross-bedded sandstone
-  conglomeratic sandstone
-  conglomerate
-  breccia
-  tuff
-  basalt
-  gneiss
-  covered interval

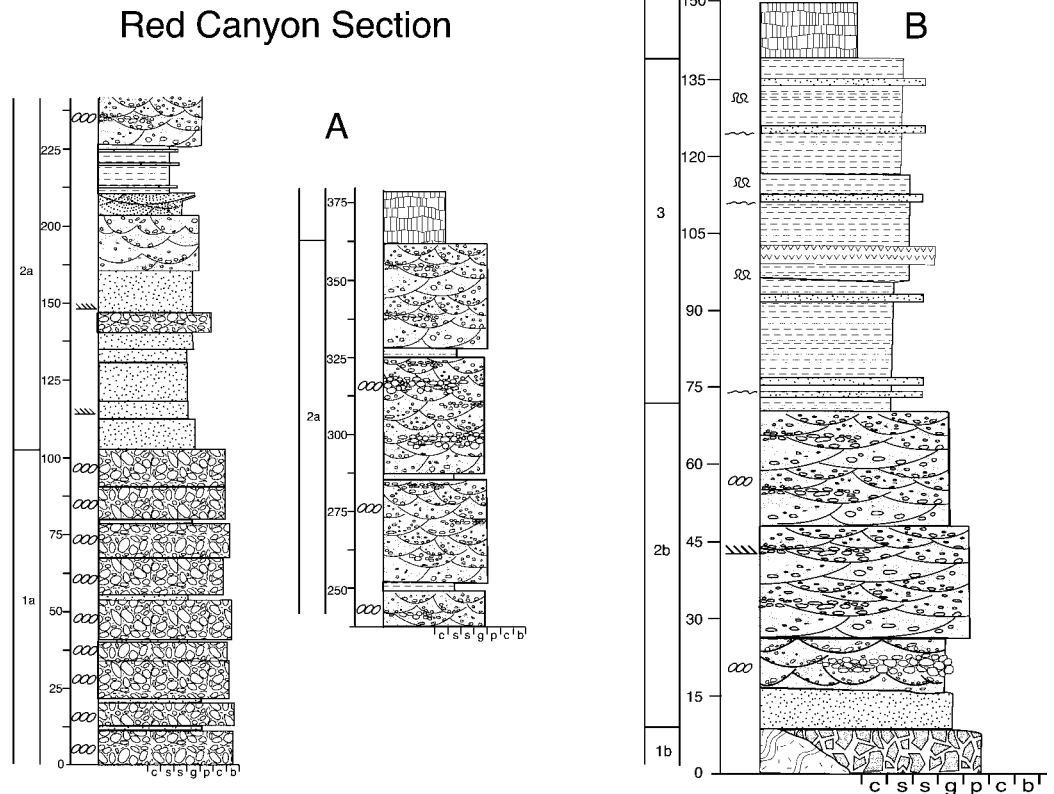


Figure 5. Measured stratigraphic sections illustrating facies associations in the lower part of Diligencia Formation. Locations of sections are indicated in Figure 3; A is from northern basin margin, B–E are from southern basin margin. Average thicknesses of facies associations are shown.

sedimentary rocks on the northern margin were deposited in high-gradient systems. Comparable proximal to medial braid-plain deposits are reported as the dominant facies in the similar-aged Soledad and Plush Ranch basins (Fig. 2) of the Transverse Range province (Hendrix and Ingersoll, 1987; Cole and Stanley, 1995), and in Miocene successions of the Basin and Range province (e.g., Sherrod and Tosdal, 1991; Fedo and Miller, 1992; Sherrod and Nielsen, 1993 and papers therein; Glazner et al., 2000). The strong south-southeast paleocurrent mode for facies association 2a (Fig. 6A), coupled with the pebble imbrication in facies association 1a (Table 1), supports a general northwest to southeast paleoslope.

Depositional processes inferred for the facies associations preserved along the southern basin margin (1b, 2b–2d) are typical of arid-region alluvial fans that underwent ephemeral flow (cf. Beaty, 1990). Matrix-supported breccia and conglomerate (1b) reflect deposition from debris flows, followed by stream-flow reworking between mass-flow events on proxi-

mal to medial fans (cf. Nemeč and Steel, 1984). Although debris-flow deposits do not make up large volumes of the total sedimentary succession, they are widespread along the southern basin margin, and thus are potentially significant paleoclimate indicators. Paleobotanical studies (Axelrod, 1950; Wolfe, 1986) indicate that the Miocene climate in this region was semiarid. Vegetation on hill slopes was probably quite sparse, and precipitation episodic. Both of these factors promote development of gravity-driven mass flows (Fisher, 1971). Stratified conglomerates and sandstones (2b, 2c) record stream-flow processes that operated on more distal parts of the fans. During flood events, flow is often great enough to overwhelm the active system of channels, and deposition occurs from unconfined sheetflood (Picard and High, 1973; Hardie et al., 1978; Nilsen, 1982). The remarkable abundance of planar-laminated sandstone in facies association 2d suggests that deposition took place below the intersection point of a fan, where stream channelization is poorly de-

veloped and unconfined flow is promoted (cf. Hooke, 1967; Nilsen, 1982). Paleocurrent data (Fig. 6, B and C) are compatible with a south to north paleoslope, and with wave reworking along a general east-west-trending shoreline. Similar associations of debris-flow, stream-flow, and sheetflood deposits are reported from the Triassic Chinle Formation in New Mexico (DeLuca and Eriksson, 1989) and the Paleocene Esplagafreda Formation of northern Spain (Dreyer, 1993), both of which developed under arid conditions.

Alluvial-fan deposits of the southern basin margin are overlain by, and interfinger with, rocks of lacustrine origin (facies association 3). The arrangement of these facies associations suggests that the southern basin margin was dominated by a system of relatively low gradient alluvial fans that extended into a playa-lacustrine basin. Abundant evaporites and desiccation features, including mud cracks, indicate that the lake system was ephemeral and supports the inferred semiarid paleoclimate. Limestone similar to that present within the

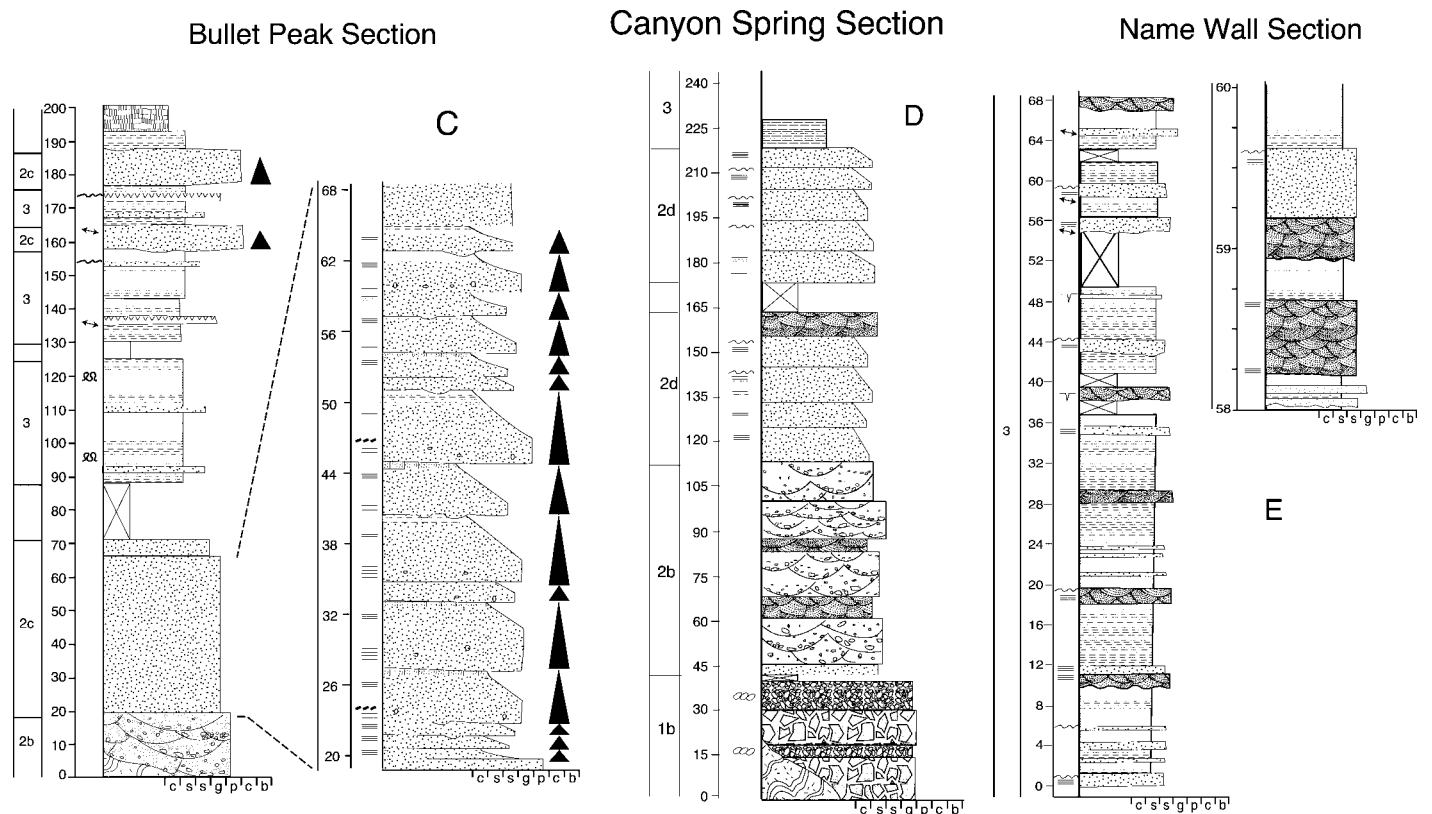


Figure 5. (Continued).

lacustrine facies association has been reported from nearby basins of similar age (Fedo and Miller, 1992). The oolitic limestone probably developed near the lake margin and the massive limestone farther offshore (cf. Swirydzuk et al., 1979). Formation of carbonate from lake water requires an unusually high ratio of dissolved bicarbonate to calcium and magnesium in the groundwater (Hardie and Eugster, 1970; Hardie et al., 1978). However, as carbonate is formed, the process removes bicarbonate from the system until the ratio is too low for further carbonate precipitation. Thereafter, calcium and/or magnesium sulfates commonly form (Hardie and Eugster, 1970; Hardie et al., 1978). This brine evolution scheme suggests that the carbonate rocks are likely to form near the margin of the lacustrine deposit, and sediments nearer the center should contain most of the sulfate evaporites. This prediction is borne out by the observation that carbonate rather than gypsum is interbedded with sandstone of the alluvial-fan system (facies associations 2b, 2c). The source of sulfate ions for gypsum precipitation is problematical in an inland lake. Either these were derived from weathering of sulfides, or they indicate periodic marine incursions into the lake.

Thick sandstone beds intercalated within the gypsiferous siltstone are interpreted as lacustrine-margin deposits. The similarity of these deposits to those of modern small flood events (cf. Karcz, 1972) suggests either that they are the result of low-volume floods, or that they represent the most distal reaches of major flood deposits in which flow energy had decreased significantly, and flow was distributed over a relatively large area of the alluvial fan. The strong component of northwestward flow for these sandstone facies (Fig. 6D) can be related either to local depositional gradients produced by the formation of tilted basement surfaces in the hanging walls of growth faults in the Bullet Peak area (Fig. 3), or to radial flow on the distal alluvial fan.

Thin sandstone beds intercalated with the lacustrine units represent subaqueous, density underflow deposits. In ephemeral saline lakes, salinity is generally very high, and formation of density currents may be rather limited. However, during periods of increased rainfall, salinity would decrease, whereas lake area and sediment supply to that lake would increase. These factors, in concert, would favor the formation of turbid density flows and the deposition of turbidite units. The thin sandstone in this facies association contains divisions that

include the modified unit Ta of Lowe (1982), overlain by Tb and Tc and capped by the Te mudstone of a traditional Bouma sequence. Probable turbidites have also been identified in association with lacustrine deposits in the Whipple and Sacramento Mountains of California (Fedo and Miller, 1992).

Basin Geometry

The depositional systems inferred for the lower Diligencia Formation can be interpreted within the general conceptual framework provided by Leeder and Gawthorpe (1987) and used to reconstruct the original basin geometry. Leeder and Gawthorpe (1987) developed a model of the patterns of sedimentation into an internally drained, continental half-graben basin, and this model has been successfully applied to the reconstruction of such basins in the Transverse Ranges, the Basin and Range province, and elsewhere (e.g., Hendrix and Ingersoll, 1987; Hamblin and Rust, 1989; Fedo and Miller, 1992; Karpeta, 1993; Cole and Stanley, 1995). In an internally drained half-graben basin, contemporaneous sedimentary successions will be demonstrably different in different parts of the basin. Facies against the relatively steep relief of the listric fault es-

TABLE 1. DESCRIPTIVE CHARACTERISTICS OF FACIES ASSOCIATIONS

Facies associations	Grain size	Depositional texture	Sedimentary structures	Paleocurrents	Vertical successions
Northern basin margin					
Boulder conglomerate (1a) (Fig. 5A)	Well-rounded clasts of mainly granite. Clasts average 50 cm in diameter but range from 1 cm to 15 m.	Framework-supported with matrix of coarse sand (Fig. 7A).	Elongate clasts are locally imbricated.	Imbrication indicates south-east flow.	Crude discontinuous layering on scale of several to tens of meters defined by horizontally stratified sandstone beds (Fig. 7A)
Conglomerate-sandstone (2a) (Fig. 5A)	Pebble to cobble conglomerate and coarse- to very coarse-grained sandstone. Minor fine-grained sandstone and siltstone.	Erosively based, tabular and broad, lensoidal channel-form depositional units. Conglomerates are lenticular (Fig. 7B).	Trough and tabular cross-stratification and planar lamination.	Cross strata and current lineations indicate flow to southeast. (Fig. 6A)	Weakly developed upward-fining successions between 1 and 8 m thick. Lower half of section mainly sandstone, upper half conglomerate and sandstone.
Southern basin margin					
Breccia-conglomerate (1b) (Fig. 5, B and D)	Angular and rounded, pebble to cobble size clasts of gneiss, granite, and vein quartz. Very coarse to coarse-grained sandstone. Mudstone with floating pebbles.	Angular clasts float in a matrix of sand and mud. Local clast alignment. Rounded clasts are framework supported.	Matrix-supported breccia beds are massive to thickly bedded. Conglomerate defines lenticular, channel-based units. Sandstone is crudely stratified.	None	Breccia and conglomerate are interbedded at meter scale and are interlayered with mudstone and sandstone.
Conglomeratic sandstone (2b) (Fig. 5, B, C, and D)	Very coarse-grained to pebbly sandstone, local pebble conglomerate. Rare mudstone and carbonate	Pebbles localized in channels as stringers or lenses within sandstone.	Common trough cross-stratification. Local tabular cross stratification and planar lamination.	Channels and cross-strata indicate general northerly flow. (Fig. 6B)	Weakly developed upward-fining cycles 1–2 m thick. Mudstone ± carbonate (see below) cap cycles.
Sandstone-siltstone (2c) (Fig. 5C)	Very coarse- to medium-grained sandstone and siltstone. Rare pebbles.	Laterally persistent, erosively based tabular depositional units. Stringers or scattered pebbles and/or mudstone clasts in coarse-grained sandstone.	Very coarse-grained sandstone crudely stratified to massive, rare cross-stratification. Finer-grained sandstone and siltstone contain planar lamination and cross-lamination.	None	Well-developed, fining-upward sandstone successions between 1 and 3 m thick capped by ~50-cm-thick siltstone and carbonate (see below) beds.
Sandstone (2d) (Fig. 5D)	Medium to fine-grained sandstone. Rare coarse-grained sandstone.	Laterally persistent bedding surfaces and depositional units.	Planar lamination predominates. Less common trough cross-stratification and ripple and climbing ripple lamination. Local wave ripples.	Symmetrical ripples indicate northeast-southwest wave oscillation. (Fig. 6C)	Uncommon fining-upward successions up to several meters thick with soft-sediment deformation structures at top capped by wave ripples.
Gypsiferous siltstone-claystone (3) (Fig. 5, B, C, D, and E)	Dark red and gray-green siltstone and/or claystone with gypsum. Coarse- to fine-grained interbedded sandstone.	Bedding defined by sharp-based, thin (1–30 cm) and less common, thick (meter-scale) sandstone interbeds. Gypsum occurs as sheets of selenite parallel to or at a high angle to bedding.	Siltstone and/or claystone are poorly laminated. Thin sandstone beds are massive at base, less commonly trough cross-stratified, and parallel-laminated and rippled in upper half. Beds are capped by mudstone. Thick sandstone beds mainly trough cross-stratified with parallel laminations and current and wave ripples at top. Beds capped by desiccated mudstone.	Cross-strata show flow to northwest. Symmetrical ripples resulted from northwest-southeast wave oscillation. (Fig. 6D)	Sandstone beds are upward fining.
Massive and oolitic carbonate (associated with 2b, 2c, 3)	Oolites to 2 cm in diameter	Tabular orange-brown beds 30–80 cm thick. Orange-brown weathering due to presence of FeO.	No discernible internal fabric. Algal mat material (?) on bedding planes.	None	None

carpment will be dominated by thick, high-gradient alluvial-fan deposits of limited areal extent (Leeder and Gawthorpe, 1987). In contrast, facies on the gently dipping surface of the hinged hanging-wall block will be dominated by thin, low-gradient alluvial fans (cones). Each of these basin-margin sedimentary systems interfingers in the basin interior with lacustrine deposits.

The asymmetric distribution of facies across the axis of the basin suggests that, in its present orientation, the early Diligencia basin can be reconstructed as an asymmetric half-graben basin that formed in response to north-south-directed extension (Fig. 8), as originally suggested by Spittler and Arthur (1982). High-gradient fans along the northern margin are interpreted to have formed against the rel-

atively steep slope of a fault escarpment. Low-gradient alluvial fans along the southern margin are interpreted to have formed on the gently dipping hanging-wall block of the half-graben. The lacustrine deposits record the presence of a playa lake complex in the basin interior. This reconstruction assumes that: (1) the basin opened at right angles to the basin margins now marked by exposed depositional

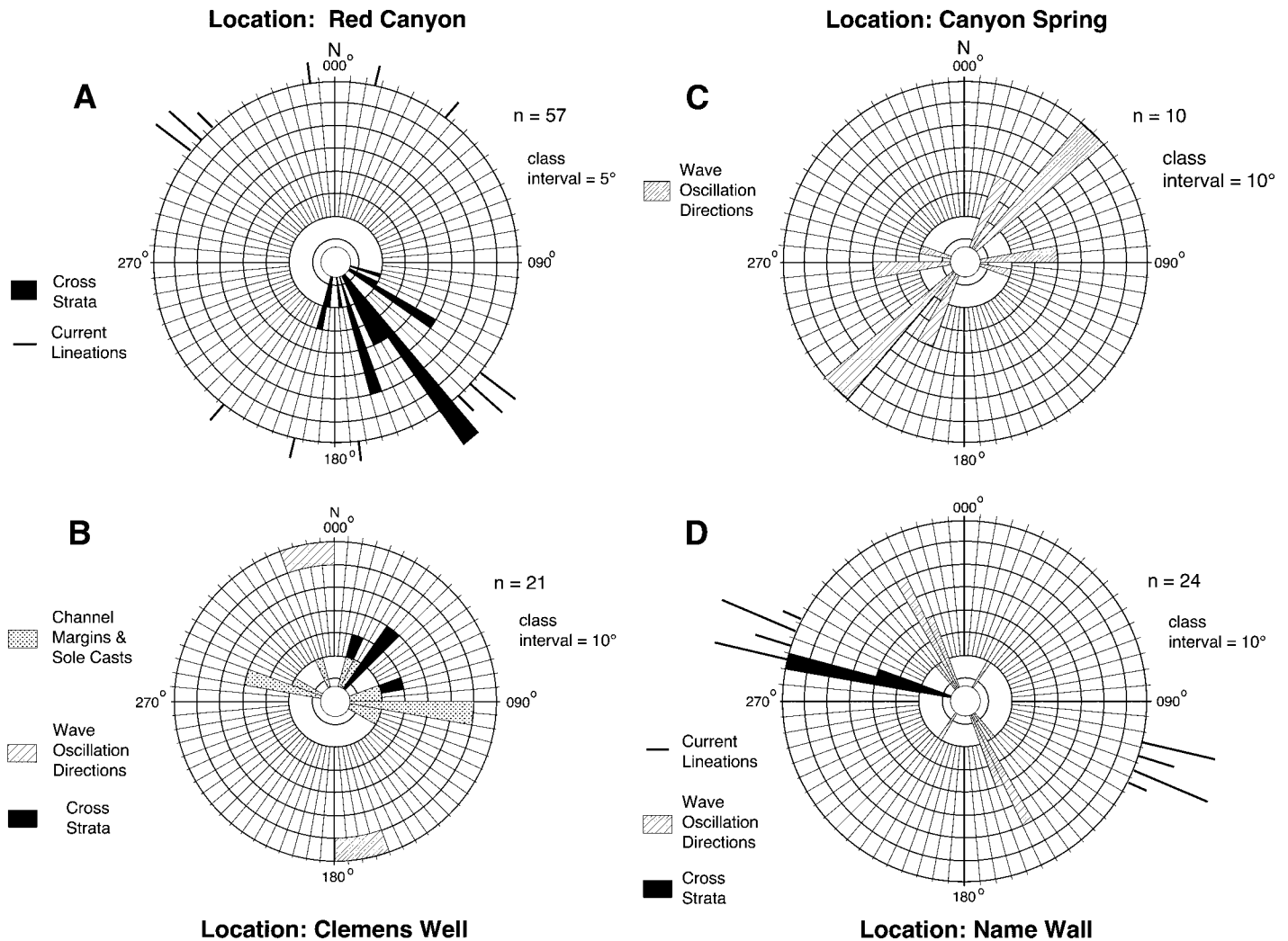


Figure 6. Rose diagrams of paleocurrent directions for Red Canyon section (northern basin margin), and Clemens Well, Canyon Spring, and Name Wall sections (all southern basin margin); see Figure 3 for locations. For tectonic dips $>15^\circ$, bedding and paleocurrent azimuths were rotated back to horizontal. Note that for clarity the two wave oscillation directions recorded in the Clemens Well section (B) are plotted at diagram margin.

contacts between the Diligencia Formation and crystalline basement rocks (Fig. 3), and (2) that the original strike of these contacts was not significantly altered during basin inversion.

The only definitive evidence for normal displacement across a fault striking parallel to the length of the basin is a thick gouge zone near the western end of the northern margin, which separates granitic basement in the footwall from breccia containing granitic clasts in the hanging wall. The fault surface is nearly horizontal; it has a gentle apparent dip toward the basin. The association of normal faulting with the northern margin strengthens the interpretation from sedimentological evidence that the basin-forming fault extended along the northern margin and dipped toward the south. The

texture and thickness of the sedimentary succession along the northern margin of the Diligencia basin indicates that the fault escarpment, against which the high-gradient alluvial fans formed, had a steep dip relative to the depositional surface on the southern margin. The presence of low-angle normal faults along this margin, in concert with the inference of a high-angle fault escarpment (now eroded away), supports the suggestion that the basin-bounding fault system had a listric geometry. However, the orientation of this inferred south-dipping normal fault at depth (i.e., high-angle versus low-angle normal faulting) is unknown (Fig. 8).

The locus of maximum extension, and thus greatest subsidence, in an asymmetric rift basin should be at the foot of the fault escarp-

ment. Thus, in the case of the Diligencia basin, the lacustrine depocenter is expected, in plan view, to be closer to the northern than the southern basin edge. Although mudstone is fairly common on the northern margin, characteristic lacustrine gypsiferous siltstone is not present. Rather, lake-bed deposits are most closely associated with the southern margin of the basin. Similar observations have been reported in Paleozoic rift basins of Nova Scotia by Hamblin and Rust (1989), who documented the widespread occurrence of lacustrine deposits in these fault-controlled basins and identified multiple playa-lake depocenters located well up on the hanging-wall ramps. The displacement of the lacustrine depocenter(s) up the hanging-wall ramp from the locus of maximum subsidence is most satisfactorily

TABLE 2. INTERPRETATION OF FACIES ASSOCIATIONS

Facies associations	Interpretation
Northern basin margin	
Boulder conglomerate (1a)	Conglomerate is similar to deposits on proximal reaches of modern gravelly braided rivers such as the Scott outwash fan and Donjek River (cf. Boothroyd and Ashley, 1975; Miall, 1977). Conglomerate represents longitudinal bar deposits and minor sandstone records bar-top deposition.
Conglomerate-sandstone (2a)	Facies are comparable to deposits of modern sandy braided rivers such as the Donjek River and the middle to lower Scott outwash fan (Boothroyd and Ashley, 1975; Miall, 1977). Conglomerate represents channel-lag deposits whereas dominant cross-bedded sandstone developed on mid-channel bars during bankfull stage. Finer-grained facies record low-stage deposition or abandonment of the flood plain.
Southern basin margin	
Breccia-conglomerate (1b)	Matrix-supported breccias beds and mudstone beds with floating pebbles represent single-event, debris-flow, and mud-flow deposits, respectively. Thick bedding reflects stacked, single-event deposits. Conglomerate records bedload reworking by stream flows (cf. Fisher, 1971; Lowe, 1979; Nemeč and Steel, 1984). Intercalated sandstone also reflects bedload reworking.
Conglomeratic sandstone (2b)	Pebble conglomerate and trough cross-beds developed in confined channels on an ephemeral braidplain, whereas planar lamination formed in response to shallow, unconfined flow (cf. Picard and High, 1973; Hardie et al., 1978; Tunbridge, 1981). Mudstone records suspension deposition following abandonment of flood plain. Vertical successions represent deposits of single, waning floods (cf. Nemeč and Steel, 1984). Weak development of cyclicity may be due to erosion of unconfined-flow deposits.
Sandstone-siltstone (2c)	Well-developed vertical successions record single, waning floods on an ephemeral flood plain. Basal massive to crudely stratified intervals with erosional bases probably represent hyperconcentrated stream-flow deposits that evolved from debris flows (cf. Nemeč and Steel, 1984). Overlying stratified sandstone and siltstone are waning, traction-current deposits.
Sandstone (2d)	Predominant planar lamination reflects unconfined, upper flow regime sheetfloods (cf. Picard and High, 1973). Upward-fining successions represent single waning flood deposits on an ephemeral flood plain (cf. McKee et al., 1967). Symmetrical ripples are generated by waves during interflow periods.
Gypsiferous siltstone-claystone (3)	Association of facies records deposition within and marginal to a playa lake. Siltstone-claystone represent suspension deposits whereas gypsum reflects hypersaline conditions favoring evaporite deposition. Assemblage of sedimentary structures in thick sandstone beds is comparable to deposits of low-discharge flash floods (cf. Karcz, 1972). Vertical succession of grain size and sedimentary structures in thin beds resemble Bouma sequences produced by waning turbid underflows (cf. Hardie et al., 1978).
Massive and oolitic carbonate (associated with 2b, 2c, 3)	Carbonate interpreted as lacustrine-margin deposits produced by inorganic precipitation in low- and high-energy settings (cf. Swirdczuk et al., 1979). Iron content probably related to secondary ankeritization.

explained by the behavior of the footwall-sourced alluvial fans. Under conditions of sediment supply exceeding subsidence, these high-gradient fans are likely to have a high rate of progradation, and accumulation rates higher than those for the lacustrine system. As these fans prograde across the basin, the active playa is likely to be pushed up the hanging-wall ramp.

ALTERNATIVE MODELS FOR MIOCENE BASIN EVOLUTION INVOLVING BASEMENT EXHUMATION

As discussed herein, facies analysis indicates that the Diligencia Formation was deposited in a half-graben basin with a steep, possibly fault-controlled, south-facing northern escarpment (Fig. 8) and a more gentle, north-facing southern slope (Spittler and Arthur, 1982). Both the facies analysis reported here and the earlier work of Spittler and Arthur (1982) indicate that deposition began (unit 1) with coarse siliciclastic input from both the north and south margins of the basin; however, the northern source supplied the coarser grained and greater quantity of sediment. Paleocurrent data for units 2 and 3, including possible landslide deposits in unit 3 (Crowell, 1993b), also indicate a northern sediment source.

In marked contrast to this facies-based interpretation for evolution of the Diligencia basin, structural, metamorphic, and radiometric cooling age data from the basement rocks to the south of the basin have previously been interpreted to indicate that the Diligencia basin developed in the hanging wall of a north-east-dipping (present-day coordinates) system of normal faults during crustal-scale Tertiary age extension and basement exhumation (Goodmacher et al., 1989; Robinson and Frost, 1989, 1991, 1996). Here we review the evidence for Tertiary basement exhumation and associated basin formation in the Orocopia Mountains, and compare these data with similar studies that have been undertaken in other basement massifs in southern California. These massifs are exposed in an arcuate belt that includes the Orocopia Mountains and extends southeastward through southeastern California from at least the San Gabriel Mountains into Arizona (Fig. 2). East of the San Andreas fault this series of basement culminations is referred to as the Chocolate Mountains anticlinorium (Haxel and Dillon, 1978; Haxel et al., 1985). Throughout this review we use present-day geographic coordinates, but note that some of these regions probably un-

derwent significant clockwise rotation about vertical axes in late Miocene to Pliocene time. Present-day compass directions given for pre-rotation features may therefore not necessarily indicate their original orientation.

Orocopia Mountains

On the southern side of the basin, the Diligencia Formation locally is in depositional contact upon a basement uplift of quartzofeldspathic augen gneiss, amphibolite, syenite, adamellite, gabbro, and anorthosite (Crowell and Walker, 1962) of Proterozoic age (Silver, 1971). Here the unconformity is vertical to locally overturned, and laterally passes eastward into a steeply dipping fault (Spittler and Arthur, 1982; Crowell, 1993b). Along the southwestern margin of the basin, the contact between the Diligencia Formation sedimentary rocks and the basement rocks is marked by the Clemens Well fault (Fig. 3).

Underlying the Proterozoic igneous and

metamorphic rocks is the Orocopia Schist, which consists of metamorphosed oceanic sedimentary and basic volcanic rocks of Mesozoic, possibly Jurassic (e.g., Dillon, 1975; Haxel, 1977; Haxel and Dillon, 1978; Crowell, 1981; Haxel et al., 1987), or Cretaceous (protolith) age (Jacobson et al., 2000). In the Orocopia Mountains the mineral assemblage of the Orocopia Schist belongs to the albite-epidote amphibolite and lowermost amphibolite facies (Jacobson and Dawson, 1995). Isotopic dating of Orocopia Schist exposed in the adjacent Chocolate Mountains (Fig. 2) indicates that this metamorphism occurred in Late Cretaceous time (Haxel and Tosdal, 1986; Jacobson, 1990). Most of the schist exhibits crystalloblastic textures, but overprinting mylonitic textures occur within a few meters to tens of meters of the contact with the overlying plate of Proterozoic rocks (Jacobson and Dawson, 1995; Robinson and Frost, 1996), and formed during retrograde greenschist facies metamorphism under decreasing pressure

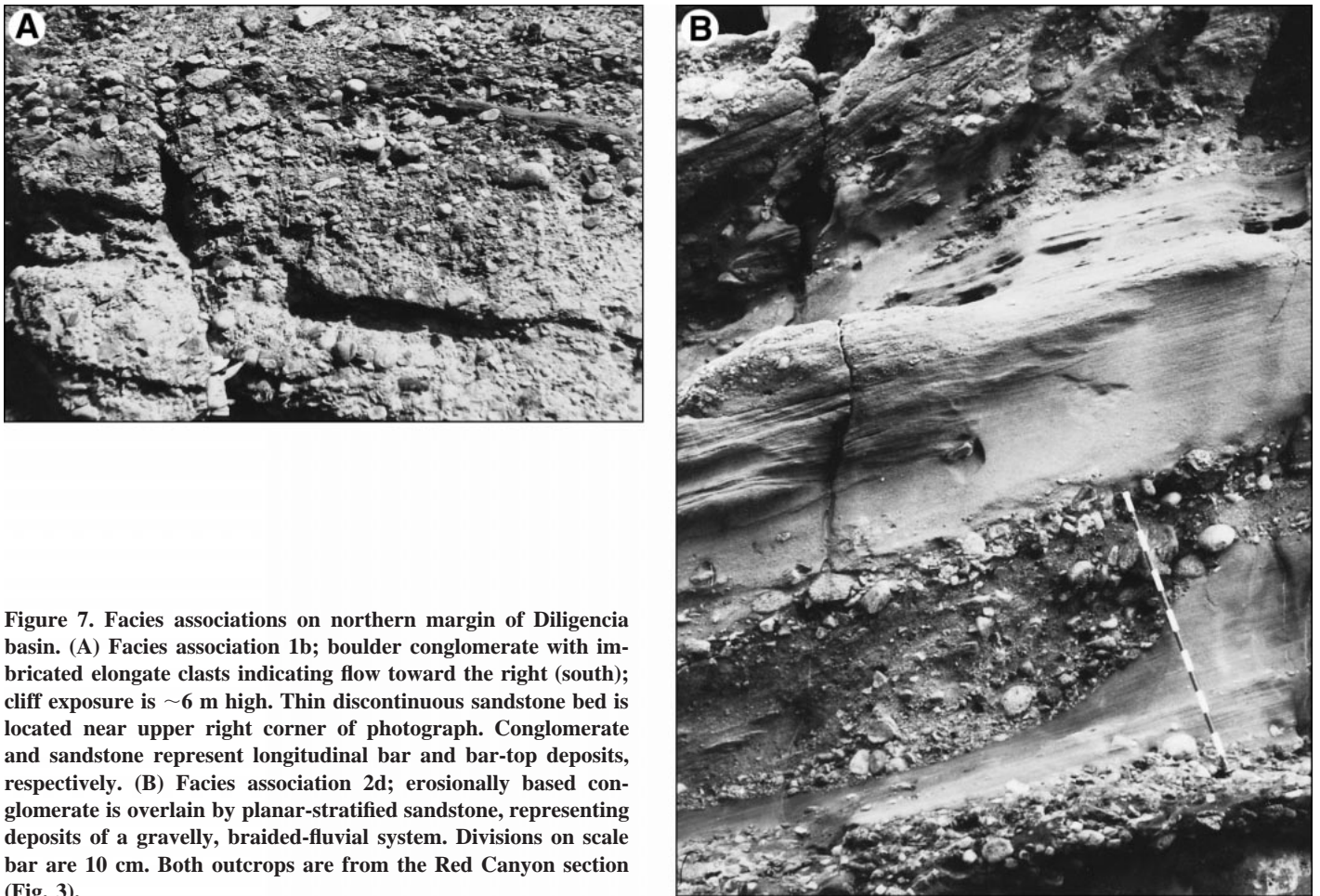


Figure 7. Facies associations on northern margin of Diligencia basin. (A) Facies association 1b; boulder conglomerate with imbricated elongate clasts indicating flow toward the right (south); cliff exposure is ~6 m high. Thin discontinuous sandstone bed is located near upper right corner of photograph. Conglomerate and sandstone represent longitudinal bar and bar-top deposits, respectively. (B) Facies association 2d; erosionally based conglomerate is overlain by planar-stratified sandstone, representing deposits of a gravelly, braided-fluvial system. Divisions on scale bar are 10 cm. Both outcrops are from the Red Canyon section (Fig. 3).

(Jacobson et al., 1987; Jacobson and Dawson, 1995). Stretching lineations in the mylonite generally plunge to the east or northeast, oblique to the north-northeast dip of the mylonitic foliation (Jacobson and Dawson, 1995, their Figs. 11 and 12; Robinson and Frost, 1996). Microstructural shear-sense indicators consistently indicate a hanging-wall down-to-the-east to northeast sense of shear (Jacobson et al., 1987; Jacobson and Dawson, 1995; Robinson and Frost, 1996). Mylonitic textures have not been observed in the upper plate rocks, although faults, fractures, and hydrothermal alteration are widespread (Goodmacher et al., 1989; Robinson and Frost, 1989, 1991; Jacobson et al., 1996; Robinson and Frost, 1996).

The gently to moderately (20° – 30° ; Robinson and Frost, 1996) northeast-dipping contact between the Orocopia Schist and the upper plate Proterozoic rocks (Fig. 3) was initially interpreted as a thrust fault and referred to as the Orocopia thrust by Crowell (1962), Ehlig (1968, 1981), Crowell (1974b), and Haxel and Dillon

(1978), although evidence for reactivation was noticed in even the earliest studies (Crowell, 1962). Robinson and Frost (1989), while accepting that late Mesozoic motion on this fault contact was in a thrust sense, suggested that the fault was reactivated as a crustal-scale normal fault during Tertiary regional extension. The hanging-wall down-to-the-east sense of motion was inferred to have led to exhumation of the underlying Orocopia Schist as a metamorphic core complex in the footwall to the fault system, and development of the Diligencia basin in the hanging wall. This interpretation was expanded upon by Robinson and Frost (1991) and Goodmacher et al. (1991) who emphasized the presence of a related anastomosing network of brittle normal faults in the upper plate Proterozoic rocks. Goodmacher et al. (1989) proposed that the Clemens Well fault, which separates the upper plate Proterozoic rocks from the Diligencia Formation to the east (Fig. 3), may also belong to this suite of normal faults, which they refer to as the Orocopia Mountains detachment system. Recent detailed remapping of the basement

rocks to the south of the Diligencia basin by Robinson and Frost (1996, their Fig. 2) indicates that the fault contact between the Orocopia Schist and the overlying plate of Proterozoic rocks (which they refer to as the Orocopia Mountains detachment fault) traced to the southeast is crosscut at a shallow angle by a brittle, more steeply dipping and more northward-striking system of normal faults referred to as the Diligencia detachment fault (Fig. 3).

A critically important step in establishing a causal relationship between movement on these basement normal faults and formation of the overlying Diligencia basin is to demonstrate that movement on the faults is synchronous with basin development. Isotopic age data for the Orocopia Mountains are very limited. Jacobson (1990) analyzed three samples from the Orocopia basement rocks: hornblende from nonmylonitic upper plate gneiss 100 m above the Orocopia Schist, muscovite from the zone of mylonitic schist, and muscovite from nonmylonitic schist ~300 m beneath the upper plate. The $^{40}\text{Ar}/^{39}\text{Ar}$ release

spectra from the three samples yielded isochron ages of 74.6 ± 0.3 Ma, 52.1 ± 0.4 Ma, and 40.6 ± 0.9 Ma respectively; only the hornblende yielded a relatively simple spectrum. Jacobson (1990) considered that the age discordance between the upper plate (older age) and lower plate (younger ages) is consistent with the kinematic evidence that the Orocopia thrust was actually a low-angle normal fault (at least in early-middle Eocene time) that excised the original thrust and juxtaposed Orocopia Schist against structurally high upper plate rocks that were cool and therefore old in terms of $^{40}\text{Ar}/^{39}\text{Ar}$ age. The age difference between the mylonitic (52 Ma) and non-mylonitic (41 Ma) schist was taken to indicate the possible presence of an additional normal fault between these two units. The 52 Ma muscovite age (middle Eocene) for the late mylonite at the top of the Orocopia Schist clearly implies (Jacobson, 1990) that normal-sense motion under greenschist facies conditions on the Orocopia Mountains detachment fault must predate detachment faulting (dated as post-22 Ma; Sherrod and Tosdal, 1991) in the Basin and Range province to the east.

Determining both the age and sense of motion on the younger brittle normal faults that cut the Orocopia Mountains detachment fault, but are confined to the basement rocks, remains problematic. Robinson and Frost (1996, p. 280) stated that microbreccia that truncates the Orocopia Mountains detachment fault has been dated as 25 Ma and that brittle fault gouge formed until 14 Ma. However, because no details are given of sample location, nature of faults sampled, minerals used, or dating techniques employed, we are unable to evaluate these data. An absolute minimum age for motion on the Orocopia Mountains detachment fault may be provided in the Chocolate Mountains to the southeast (Fig. 2), where a fault contact at the top of the Orocopia Schist, which may represent the along-strike equivalent of the Orocopia Mountains detachment fault, is cut by early Miocene hypabyssal intrusive rocks (Dillon, 1975).

Although clasts of upper plate Proterozoic rocks are commonly found in the Diligencia Formation, no clasts of Orocopia Schist have been recorded, indicating that at least adjacent to the developing Diligencia basin, the Orocopia Schist had not been unroofed by late Oligocene to early Miocene time (Crowell, 1975; Spittler and Arthur, 1982). Jacobson et al. (1996) proposed that the Orocopia Schist was brought from metamorphic depths to shallower crustal levels during Late Cretaceous to early Tertiary time; middle Tertiary extension on brittle faults was responsible for bringing

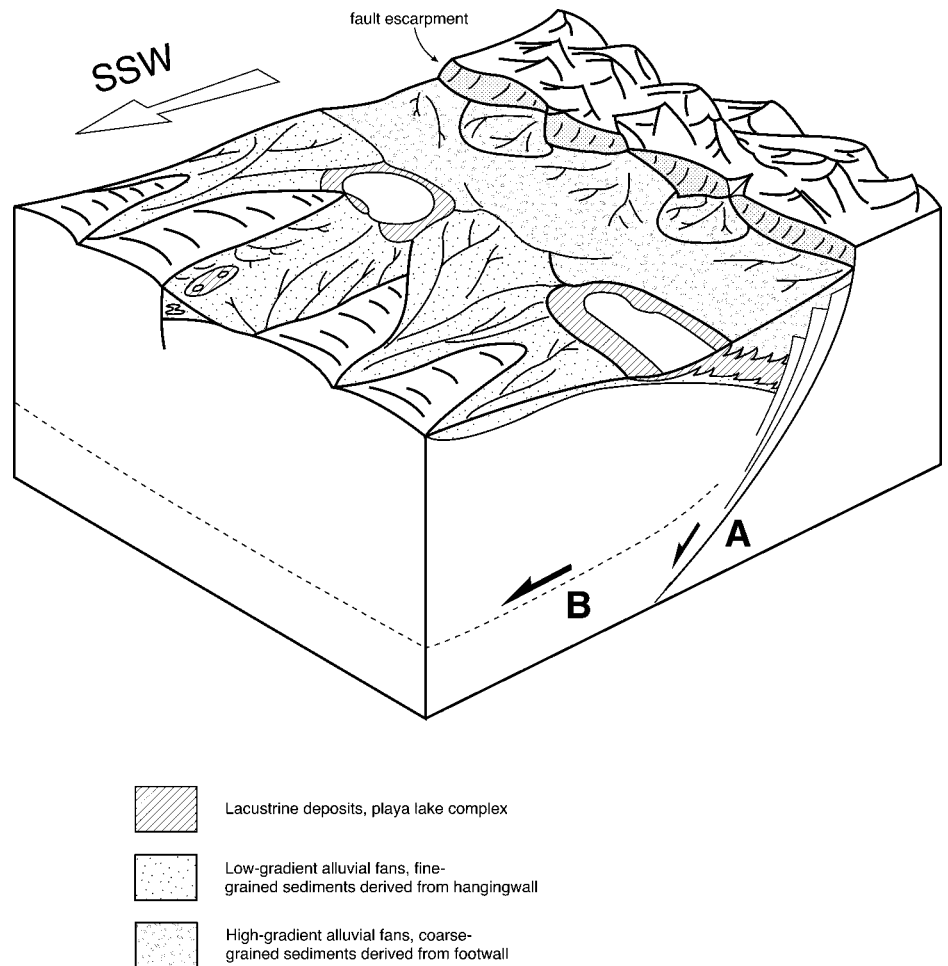


Figure 8. Block diagram illustrating proposed paleogeographic reconstruction of the early Diligencia basin, in present-day geographic coordinates. Series of south-dipping fault blocks, overlain by younger strata, and developing progressively northward during basin evolution, are included to explain observed contact between Diligencia Formation and underlying rocks on northern basin margin (Figs. 3 and 4). Alternative interpretations of south-dipping basin-controlling listric extensional fault at depth (A—high-angle normal fault, B—low-angle detachment fault) are schematic. Not to scale.

them to just below ground surface. A similar model was proposed by Robinson and Frost (1996) and linked with formation of the Diligencia basin in the hanging wall to the northeast-dipping fault system. However, both the absolute timing and magnitudes of dip-slip displacement on the late brittle faults remains unclear. Although many late brittle faults disrupt the contact between the Diligencia Formation and the basement crystalline rocks on the southern margin of the basin, the basal Miocene strata can still locally be found in depositional contact with the basement rocks (Fig. 3), demonstrating that the contacts are not major normal faults. Similar northeastward-dipping depositional contacts exposed in

the Chocolate Mountains between Tertiary strata and crystalline basement were cited by Sherrod and Tosdal (1991) and Richard (1993) as evidence against sedimentation being controlled by large-magnitude displacement on northeastward-dipping normal faults.

Chocolate Mountains Anticlinorium

Outcrops of the Orocopia Schist define a curving zone of regional-scale basement uplift referred to as the Chocolate Mountains anticlinorium (e.g., Haxel and Dillon, 1978, 1985; Richard, 1993), which extends southeastward from the Mecca Hills and Orocopia Mountains through the Chocolate Mountains, Gavilan

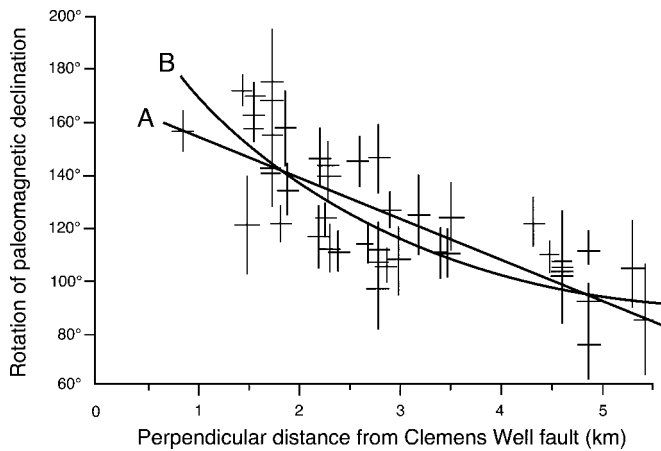


Figure 9. Diagram showing rotation of paleomagnetic declinations measured from basalt of the Diligencia Formation, plotted with respect to distance from the Clemens Well fault zone (after Terres, 1984). Rotation of declinations increases with proximity to the fault zone. A and B are linear and nonlinear regressions through the data, respectively.

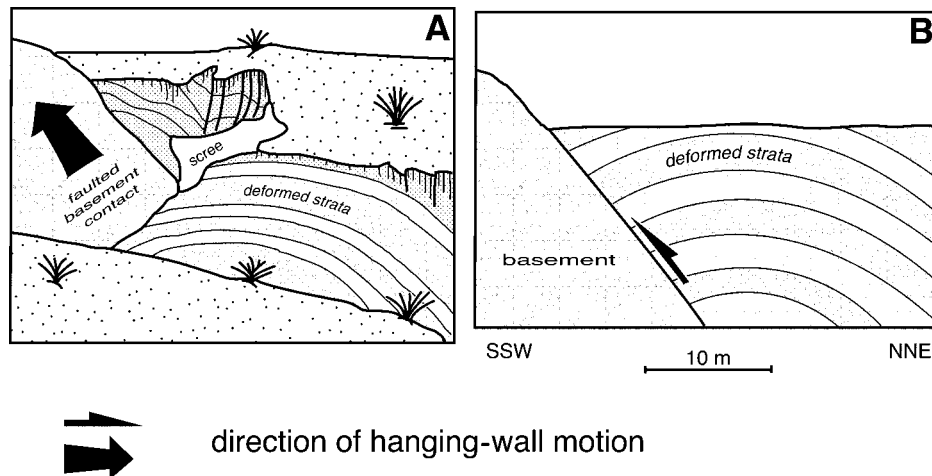


Figure 10. Nonconformity between Diligencia Formation and crystalline basement exposed in canyon on the southern margin of basin near Clemens Well Saddle section (Fig. 3). (A) Three-dimensional field sketch (viewed toward the west) and (B) cross section through segment of basement contact (nonconformity), which has been activated as a reverse fault. Arrow in A is on basement-cover contact; in fresh outcrop this is marked by a 5–20-cm-thick zone of fault gouge; the cover rocks in hanging wall of contact have been moved upward relative to basement, as indicated by large arrow.

Hills, and Trigo Mountains into Arizona (Fig. 2). To the northwest (Fig. 2), the Orocopia Schist has been correlated with the Pelona Schist and the Rand Schist (e.g., Ehlig, 1958, 1968, 1981; Crowell, 1962, 1968, 1981; Haxel and Dillon, 1978; Burchfiel and Davis, 1981; Jacobson et al., 1988). Outcrops of the Pelona and Rand schists (Fig. 2) may represent the northwestward continuation of the Chocolate Mountains anticlinorium, now offset by the San Andreas fault system.

The Rand, Pelona, and Orocopia Schists consist of oceanic rocks that underlie North American continental basement along the Rand, Vincent, Orocopia, and Chocolate Mountains faults (Ehlig, 1958, 1981; Haxel and Dillon, 1978; Jacobson et al., 1996, 1998). The schists were subjected to high-pressure metamorphism in Late Cretaceous–early Tertiary time, and are considered by many to be correlatives of the Franciscan complex emplaced beneath North America

during east-dipping subduction (e.g., Crowell, 1968, 1981; Burchfiel and Davis, 1981; Jacobson and Dawson, 1995; Jacobson et al., 1996). This interpretation conflicts, however, with local evidence for northeast transport of the overlying upper plate crystalline rocks in the Rand Mountains (Postlethwaite and Jacobson, 1987), San Gabriel Mountains (Ehlig, 1958, 1981), Orocopia Mountains (Jacobson et al., 1987; Jacobson and Dawson, 1995; Robinson and Frost, 1996), Chocolate Mountains (Haxel and Dillon, 1978; Ehlig, 1981; Tosdal et al., 1986; Dillon et al., 1990), and Gavilan Hills (Simpson, 1986, 1990; Oyarzabal et al., 1997).

In order to resolve this dilemma, most workers now consider that northeast movement of the upper plate rocks occurred during later extensional reactivation of an earlier thrust system, referred to as the Vincent–Chocolate Mountains thrust system by Haxel and Dillon (1978), that may have been related to subduction (see also Burchfiel and Davis, 1981; Crowell, 1981; Frost et al., 1981; Frost and Martin, 1983; Hamilton, 1987; Richard and Haxel, 1991; Jacobson et al., 1996). However, the age of extensional movement on the system of faults that separates the Rand, Pelona, and Orocopia Schists from the upper plate Precambrian and Mesozoic crystalline rocks remains uncertain (see review by Jacobson et al., 1996). Frost et al. (1981), Frost and Martin (1983), Hamilton (1987), and Bishop and Ehlig (1990) proposed that extensional reactivation on the Vincent–Chocolate Mountain thrust occurred largely during middle Tertiary time. This is consistent with both the widespread occurrence of middle Tertiary extension recognized in southern California, and the first appearance of the Pelona and Orocopia Schists as sedimentary clasts in early to middle Miocene successions in the southern San Joaquin basin (Goodman and Malin, 1992), Soledad basin (Ehlert, 1982; Hendrix, 1993), and Chocolate Mountains (Dillon, 1975; Hughes, 1993). As discussed here, however, clasts of Orocopia Schist have not been recorded in the Diligencia basin. Sherrod and Tosdal (1991) inferred that the Chocolate Mountains thrust remained unbreached by erosion and faulting until middle Miocene time, because lower and middle Tertiary units are nowhere observed in depositional contact with the Orocopia Schist, despite its widespread distribution in areas containing thick sections of lower and middle Tertiary strata. Large-scale Tertiary age extensional reactivation of the Vincent–Chocolate Mountain thrust system is not generally supported by isotopic dating of metamorphic rocks located

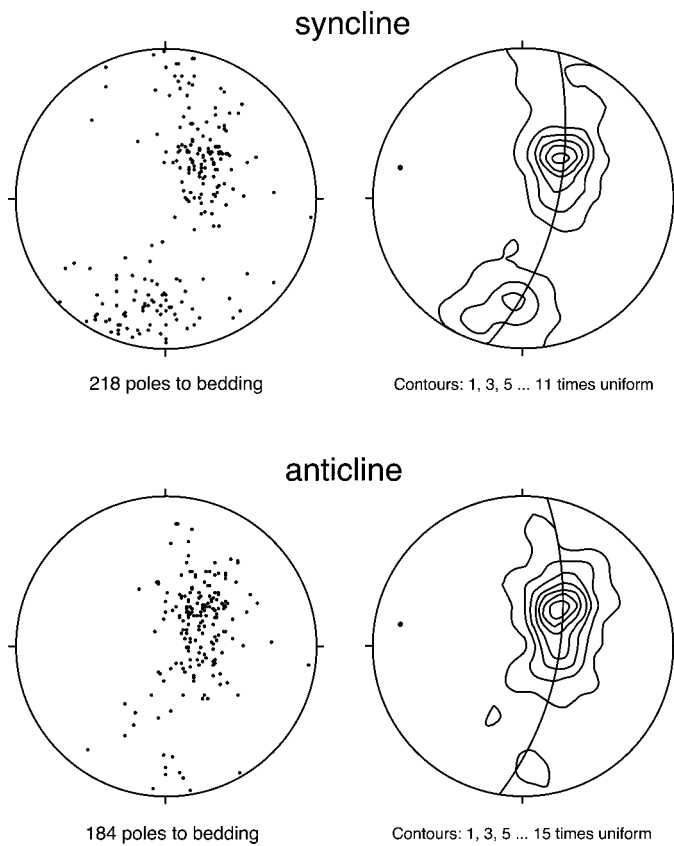


Figure 11. Structural analysis of the major syncline-anticline fold pair in Diligencia Formation strata adjacent to southern basin margin; poles to bedding are plotted on equal-area nets using the computer program Stereonet (Manktelow, 1989). Best-fit fold profile plane and fold axis are indicated in each contoured diagram.

close to the fault system. The $^{40}\text{Ar}/^{39}\text{Ar}$ cooling ages of phengite and amphibole from schist in the Rand, San Gabriel, and Chocolate Mountains, as well as the Orocochia Mountains, are rarely younger than 50 Ma (Jacobson, 1990), indicating that cooling occurred soon after presumed prograde metamorphism and long before middle Tertiary extension in southern California (Jacobson et al., 1996). To date, the only documented isotopic evidence for possible Tertiary age motion on the Vincent-Chocolate Mountain fault system that we are aware of to the southeast of the Diligencia basin is in the Gavillan Hills (Fig. 2) where Oyarzabal et al. (1997) obtained apatite fission track ages of 18–19 from two samples of Orocochia Schist and one sample of upper plate rock. To the northwest of the Diligencia basin in the western San Gabriel Mountains (Fig. 2) Cummings et al. (1982) obtained apatite fission track ages of 17.5 ± 2.1 Ma, indicating uplift and cooling of basement rocks 6 to 9 million years after initiation of the Soledad basin at approximately 25 ± 1 Ma (Frizzell

and Weigand, 1993; Hendrix, 1993). In contrast, recently published apatite fission track and (U-Th)/He analyses by Blythe et al. (2000) from the western San Gabriel Mountains indicate that a significant period of cooling began at approximately 23 Ma and continued until approximately 12 Ma. Regardless of the exact age for onset of uplift/cooling, however, Jacobson et al. (1996) have pointed out that all confirmed middle Tertiary extensional faults in the vicinity of the Chocolate Mountains anticlinorium are shallow, brittle features with maximum offsets of a few kilometers rather than tens of kilometers (cf. interpretation of seismic data by Morris, 1993). In addition, although numerous brittle faults disrupt the contact, basal Tertiary strata can be found in depositional contact with the underlying pre-Tertiary upper plate rocks in many places (including the Orocochia Mountains), demonstrating that the faults between these rocks are not major normal faults (Sherrod and Tosdal, 1991; Richards, 1993).

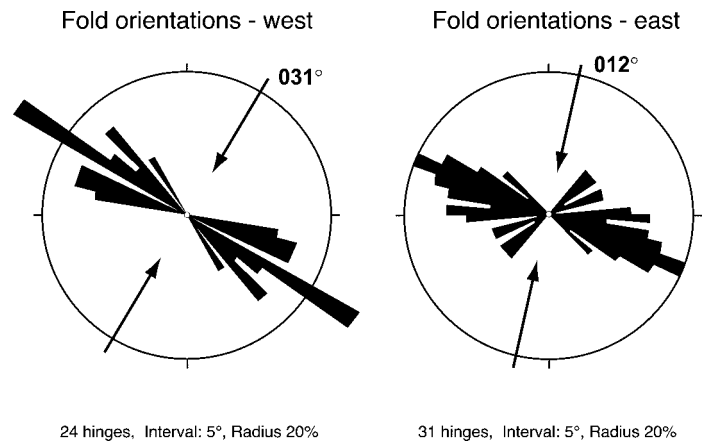


Figure 12. Circular histogram plots of fold-hinge trends from the western and eastern parts of the Diligencia basin. The direction of maximum horizontal contraction direction (represented by arrows) is inferred to be oriented perpendicular to the vector mean of the hinge trends. See text for discussion.

BLOCK ROTATION AND COMPARISON WITH OTHER MIOCENE AGE BASINS

Regional Framework

Paleomagnetic data indicate that the eastern Transverse Ranges have undergone $\sim 41^\circ \pm 7^\circ$ of clockwise rotation about a vertical axis since late Miocene time (Carter et al., 1987); this inferred clockwise rotation may be supported by a change in strike of the Jurassic age Independence Dike swarm across the region (cf. Ron and Nur, 1996, 1997; Howard and Hopson, 1997). In contrast, paleomagnetic data from the western Transverse Ranges indicate that $\sim 90^\circ$ of clockwise rotation has occurred since early Miocene time (Hornafius et al., 1986, and references therein). Carter et al. (1987) suggested that crustal rotation of the eastern Transverse Ranges began later and is of lesser magnitude than that of the western Transverse Ranges. Tectonic models proposed to explain these inferred clockwise rotations differ in detail (e.g., Luyendyk, 1980, 1991; Carter et al., 1987; Nur et al., 1993; Richard, 1993; Humphreys and Weldon, 1994; Dickinson, 1996), but all are based on the general concept that rotation of elongate crustal blocks has occurred in response to a northwest-striking dextral shear couple resulting from Pacific–North American plate interaction. Also central to all the models is the concept that brittle crustal blocks must be detached at depth (Cox, 1980; Jackson and Molnar, 1990), and allowed to translate and rotate clockwise about a near vertical axis above this detach-

ment surface in response to distributed dextral and sinistral shear on the currently northwest- and east-striking strike-slip faults, respectively (Figs. 1 and 2), that bound the individual crustal blocks.

The currently east-west-trending crustal block containing the Diligencia basin is bounded to the north and south, respectively, by the Chiriaco and Salton Wash faults, to the east by the Sheep Hole fault, and to the west by the San Andreas and Clemens Well faults (Fig. 2). In chronological order, the degree of clockwise rotation predicted by the various tectonic models for this crustal block is: 70°–80° (Luyendyk et al., 1980), 60° (Carter et al., 1987, their Fig. 7), 41° (Luyendyk, 1991), 55° (Nur et al., 1993, their Fig. 3), and 45° (Richard, 1993, his Fig. 8). Dickinson (1996) assumed an average clockwise rotation of $44^\circ \pm 7^\circ$ for currently east-west-trending crustal blocks in his modeling of the eastern Transverse Ranges.

Although an episode of early Miocene clockwise rotation has been identified east of the San Andreas fault in the Tehachapi block and northern Mojave Desert (Ross et al., 1989; Wells and Hillhouse, 1989; Luyendyk, 1991; Dokka et al., 1998), Richard (1993) regarded rotation of the eastern Transverse Ranges as being bracketed between 10 ± 2 Ma and 4.5 ± 0.2 Ma. Basalts as young as 10 ± 2 Ma in the eastern Transverse Ranges record the full paleomagnetic declination observed (Carter et al., 1987). In contrast, basalt lava flows south of the eastern termination of the east-west-striking Blue Cut fault, which have been dated as 4.5 ± 0.2 Ma, appear to overlap the trace of the north-northwest-striking Sheep Hole fault (locations shown in Fig. 2), and paleomagnetic data indicate that they have either not been rotated (Richard, 1993) or that opposing shear senses on the two faults resulted in no net rotation at this locality (Carter et al., 1987). The precise timing of the onset and cessation of strike-slip faulting and associated block rotation remains uncertain. For example, dextral displacement along the intra-Mojave faults are definitely post 13.5 Ma, but may have begun as late as 6 Ma (Dokka and Travis, 1990a). Luyendyk (1991) suggested that block rotation of the eastern Transverse Ranges may have begun ca. 6.5 Ma and is continuing to the present day.

Paleomagnetic Data for the Diligencia Basin: Implications for Original Basin Configuration and Correlation with Regional Extension

Paleomagnetic declinations preserved in basalt of the Diligencia Formation indicate an

apparent clockwise rotation of as much as 175° (Terres et al., 1980; Terres, 1984; Luyendyk et al., 1985; Carter et al., 1987). However, much of this anomalously large apparent rotation is probably local because Cretaceous dikes and lava flows of late Miocene and Pliocene age located in the Eagle and Pinto Mountains, 30 km north of the Diligencia basin, all indicate regional clockwise rotation of $\sim 40^\circ$ since late Miocene time (Terres, 1984; Luyendyk et al., 1985; Carter et al., 1987).

Paleomagnetic declinations preserved in the Diligencia basin vary systematically with distance from the Clemens Well fault (Fig. 9). Declinations near the center of the basin indicate that the crustal block containing the Diligencia basin may have been rotated by no more than 110° about a vertical axis since deposition ceased. Declinations closer to the fault zone are increasingly rotated in a clockwise direction with respect to those data farther from the fault (Terres, 1984). The difference between the declinations closest to the Clemens Well fault and those farthest from the fault is 80°–115°. If the declinations are considered as passive linear markers, and the difference in orientation is assumed to be due to rotation into a dextral strike-slip fault zone, then shearing must be responsible for as much as 100° of clockwise rotation. Whereas both the fold hinge and fault strike data (discussed in the following) also exhibit apparent clockwise rotation into the fault zone (Fig. 3), the amount of rotation is more than five times greater in the paleomagnetic data. This apparent paradox may be explained by a large amount of the rotation taking place before initiation of folding and faulting (Terres, 1984).

Paleomagnetic studies of basalt in the Diligencia Formation indicate that although the Diligencia basin is currently an east-west elongate trough (Fig. 3), the present-day orientation may not accurately reflect the orientation during basin formation. If the crustal block containing the Diligencia basin has rotated clockwise $\sim 90^\circ$, then rotating the block back 90° counterclockwise indicates that the basin may have formed in response to east-west-oriented extension (Terres, 1984), as a north-south elongate trough above an east-dipping normal fault. An $\sim 45^\circ$ clockwise rotation, as assumed in most of the tectonic models for the eastern Transverse Ranges, would suggest that the basin was originally oriented northeast-southwest and formed in response to southeast-northwest extension above a southeast-dipping fault. Neither of these inferred extension directions for the Diligencia basin is parallel to the early Miocene northeast-southwest (N50°–60°E) extension direction for the

adjacent sector of the Basin and Range province (Glazner and Bartley, 1984; Wust, 1986; Best, 1988; Dokka and Ross, 1995), casting doubt on whether the Diligencia basin formed in response to Basin and Range extension.

This reconstruction assumes, however, that the basin opened at right angles to the apparent basin margins now marked by exposed depositional contacts between the Diligencia Formation and crystalline basement rocks (Fig. 3), and that the original strike of these contacts was not significantly altered during folding and faulting associated with basin inversion. As described here, paleocurrent data, particularly from cross-beds on the northern basin margin, indicate flow toward the southeast to south-southeast (Fig. 6A; Table 1), oblique to the mapped basin margin (Fig. 3). A 90° counterclockwise restoration would indicate an original current direction toward the northeast and east-northeast, i.e., subparallel to the extension direction for the adjacent sector of the Basin and Range province. Note that the initial stages of formation of the Diligencia basin, in either latest Oligocene or earliest Miocene time, ca. 24 Ma, slightly predate initiation of major low-angle extension deformation at 22–21 Ma recognized in adjacent parts of the Basin and Range to the east (Sherrod and Tosdal, 1991; Stewart, 1998), and extension directions may have been different at this time.

Robinson and Frost (1996) suggested that currently eastward-plunging slickensides on brittle normal faults that crosscut the mylonite of the Orocopia Mountains detachment fault (Fig. 3) are associated with formation of the adjacent Diligencia basin and, assuming an $\sim 45^\circ$ clockwise rotation, may have originally formed in response to northeast-directed Basin and Range extension. However, apart from postdating the early-middle Eocene age mylonite (Jacobson, 1990), the age of these brittle faults, and therefore their relationship to formation of the Diligencia basin, remains uncertain.

Correlation of the Diligencia basin with extensional structures west of the San Andreas fault in southern California is complicated by post-Miocene strike-slip displacement on the San Andreas fault and earlier faults, controversy over the age of the extensional structures, and by the possibility of differential rotation between adjacent crustal blocks. In a review of these extensional structures, Axen and Fletcher (1998) argued that the dominant phase of detachment faulting was latest Miocene–Pleistocene in age and entirely, or almost entirely, postdated Basin and Range-style detachment faulting in the lower Colorado River region to the east.

Comparison with Miocene Basins West of San Andreas Fault

Based on physical and temporal similarity, the Diligencia basin is considered by some (e.g., Crowell, 1960, 1962; Crowell and Walker, 1962; Bohannon, 1975; Powell, 1981, 1993; Tennyson, 1989; Crowell, 1993a; Frizzell and Weigand, 1993) to have been originally contiguous with the Soledad and/or Plush Ranch basins now located to the northwest of the Diligencia basin on the western side of the San Andreas fault (Figs. 1 and 2). Offset of one basin from another is thought to have occurred by regional-scale dextral strike-slip displacement on the San Andreas and San Gabriel faults, and precursor faults such as the Clemens Well–Fenner–San Francisquito fault (e.g., Powell, 1981; Powell and Weldon, 1992; Dillon and Ehlig, 1993; Matti and Morton, 1993; Powell, 1993; Weldon et al., 1993). A detailed discussion of the various models proposed for late Cenozoic strike-slip faulting in southern California and their implications for palinspastic restoration is beyond the scope of this paper. Here we simply discuss two of the more commonly cited palinspastic restorations and their relationships to our interpretation of the original geometry of the Diligencia basin.

Bohannon (1975) suggested that before ~60 km of dextral slip along the San Gabriel fault, and ~240 km of dextral slip on the San Andreas fault, the Plush Ranch, Soledad, and Diligencia basins were originally aligned in a west-east belt, the Soledad basin being located between the Diligencia basin (to the east) and the Plush Ranch basin (to the west). This palinspastic restoration was followed by Tennyson (1989), who further suggested that the Cuyama basin (Fig. 1) may originally have been positioned at the western end of this east-west alignment of early Miocene basins. Powell (1981) proposed an alternative reconstruction in which early dextral strike-slip motion (~80 km) occurred on a precursor fault (now marked by the Clemens Well, Fenner, and San Francisquito faults; Fig. 2), which was then crosscut, and the individual segments displaced, by the evolving San Andreas fault system. In Powell's model ~240 km of slip is assigned to the combined San Andreas and San Gabriel faults (Matti and Morton, 1993), and the Diligencia basin is restored to a position adjacent to and directly east of the Plush Ranch basin, the Soledad basin originally occupying a position to the southeast of the Plush Ranch–Diligencia composite basin. A more detailed review of the palinspastic restorations proposed by Bohannon (1975) and

Powell (1981), which in their original form did not take into account the block rotations indicated by paleomagnetic data, was given by Frizzell and Weigand (1993).

Original contiguity between the Diligencia basin and either the Soledad or Plush Ranch basins is not supported by paleomagnetic data. Data for the Diligencia Formation from both lava flows and interbedded strata indicate a clear inclination anomaly (low inclination), whereas results from the Soledad and Plush Ranch basins do not (Luyendyk et al., 1985, p. 12461). Original contiguity among the basins also seems unlikely based on integration of the facies analysis and declination data. As discussed here, our facies and paleocurrent analyses have demonstrated that, in present-day coordinates, the Diligencia basin was characterized by a steep northern margin flanking a fault escarpment, and a gentle, hinged southern margin (Fig. 8). In contrast to the Diligencia basin, the Plush Ranch basin had a steep southern margin with the northern margin developed on the hanging wall block of a listric fault (Cole and Stanley, 1995). Opposing polarities are common in rift systems, e.g., as in the East African Rift where adjacent half-grabens of opposite polarity are separated by accommodation zones (Rosendahl, 1987). However, paleomagnetic declination data from the Diligencia and Plush Ranch basins (Terres, 1984; Luyendyk et al., 1985) indicate that whereas the Diligencia basin may have been rotated clockwise by ~90° since late Miocene time (or 40°–45° as assumed in tectonic models of Luyendyk, 1991; Richard, 1993; and Dickinson, 1996), the Plush Ranch basin has undergone only 6° of counterclockwise rotation. Thus, following palinspastic restoration, the long axes of the Diligencia and Plush Ranch basins would have been at a high angle with respect to each other, the Diligencia basin opening to the east or southeast and the Plush Ranch basin opening to the north.

The Soledad basin, like the Plush Ranch basin, is also considered to have had a steep southern margin in present-day coordinates (Hendrix and Ingersoll, 1987; Hendrix 1993), but paleomagnetic data indicate that the Soledad basin has undergone ~37° of clockwise rotation (Terres and Luyendyk, 1985). Following palinspastic restoration, the Soledad basin would have opened to the northwest, in contrast to the Diligencia basin, which opened to the east or southeast. Thus, it is difficult to reconcile the inferred tensional stress field responsible for formation of the Diligencia basin with those that produced the Plush Ranch and Soledad basins. Similarly, it is difficult to reconcile the inferred opening directions of these

Miocene basins (Diligencia basin—east or southeast, although paleocurrent data discussed here suggest opening to the northeast; Soledad basin—northwest; Plush Ranch basin—north) with the contemporaneous northeast-southwest (N50°–60°E) extension direction for the adjacent sector of the Basin and Range province.

Clearly a steep southern or southwestern margin to the Diligencia basin (as suggested by Robinson and Frost, 1989, 1991, 1996) would be easier to reconcile with an original connection between the Diligencia basin and either the Plush Ranch or Soledad basins, but this seems to be ruled out by our facies analyses. In addition, palinspastic restoration models that include major dextral strike slip on the Clemens Well–Fenner–San Francisquito fault (e.g., Powell, 1981, 1993; Powell and Weldon, 1992; Matti and Morton, 1993) indicate that evolution of the Diligencia basin may be unrelated to extensional movement on the currently adjacent northeast-dipping Orocopia Mountains detachment fault and Diligencia detachment fault (Fig. 3), as proposed by Robinson and Frost (1996), because the Orocopia Mountains would have been located ~60–115 km to the southeast of the Diligencia basin at 16–20 Ma (see palinspastic restorations by Matti and Morton, 1993, p. 137–139).

BLOCK ROTATION AND BASIN INVERSION STRUCTURES

Inversion tectonics involves a switch in tectonic mode from extension to contraction (or vice versa), such that extensional basins are contracted and become regions of positive structural relief (McClay, 1995; see also papers in Cooper and Williams, 1989; Buchanan and Buchanan, 1995). The sedimentary rocks of the Diligencia Formation were deposited during Basin and Range extension, and subsequently deformed during north-south contraction into a series of upright kilometer-scale east-west— to northwest-southeast—trending folds, crosscut by northwest- and northeast-striking faults (Figs. 3 and 4). Hinge lines of the folds are offset by the largest of the northeast-striking faults by as much as 1 km with a dominantly sinistral shear sense (Crowell, 1975), and the lateral offset of steeply dipping hinge surfaces (cf. Figs. 3 and 4) indicate a dominant strike-slip motion.

The southern sediment-basement contact has been activated under contraction as a reverse fault along several segments of its length. In addition, a system of reverse faults parallel to the southern margin is inferred

from bedding orientations, which appear to represent thrust culmination cut-off angles. Along segments of the sediment-basement contact that have been activated under contraction, the sedimentary strata have detached at the contact with basement, and reverse separation has occurred between the rocks on each side of the active contact. Activated segments of the southern contact are generally only several tens of meters long and are always defined by a layer of fault gouge concordant to the basement surface. One structurally activated segment of the contact is significantly longer than any other and is defined not only by a thick gouge zone, but also by anticlinal folding of the strata above the contact (Fig. 10).

Clemens Well, Chiriaco, and Salton Creek Fault Zones

The northwest-southeast-striking Clemens Well fault cuts across the folded sedimentary rocks of the Diligencia basin, juxtaposing the Miocene sedimentary rocks against crystalline basement (Fig. 3). The fault can be traced for more than 20 km along strike (Crowell and Walker, 1962; Jennings, 1967), and although nowhere exposed in cross section, the locally straight map pattern suggests that it has an approximately vertical dip. Topographically, the fault is defined by a linear canyon 50–150 m wide. The fault zone is generally covered by recent gravel in the canyon floor, but where it is more readily observable, the zone appears to be fairly discrete, no more than 25 m wide. Slivers of basalt associated with the Diligencia Formation have been caught up in the fault zone and indicate a minimum dextral displacement of 900 m across the Clemens Well fault (Crowell, 1975; Spittler and Arthur, 1982).

The direction, sense, and magnitude of motion along the Clemens Well fault are controversial (see review by Richard, 1993). Crowell (1962, p. 28) originally suggested that the fault constituted part of the San Andreas fault system with “relatively small” dextral displacement, but in a later paper concluded that displacement on the fault was perhaps as much as “several tens of kilometers” (Crowell, 1975, p. 108). Powell (1981) suggested that the Clemens Well fault may represent one section of a fundamental regional scale dextral strike-slip fault system (now marked by the Clemens Well, Fenner, and San Francisquito faults; Fig. 2) that was contemporaneous with early motion on the San Andreas fault northwest of the Transverse Ranges, but preceded development of the San Andreas fault system in southern California (see also Powell and

Weldon, 1992). Powell (1981) presented a palinspastic restoration that called for 85–90 km of dextral strike slip on the Clemens Well–Fenner–San Francisquito fault; in a revised palinspastic restoration this was subsequently amended to 110 km of dextral strike slip (Powell, 1993, p. 31). Powell (1981) projected the Clemens Well–Fenner–San Francisquito fault into the Lower Colorado River region between the Chocolate and Little Chuckwalla Mountains. The along-strike continuation of this proposed fault system southeast of the mapped position of the Clemens Well fault (Fig. 2) is problematic, however, thereby casting some doubt on the validity of these large slip estimates. For example, Sherrod and Tosdal (1991) considered that their mapping of volcanic terrains in this region precludes the possibility that the projected southeastern extension of the Clemens Well fault could have had large-magnitude strike-slip motion since early Miocene time. Both the east-west-striking Chiriaco and Salton Creek faults (Fig. 2) appear to displace, or deflect, the inferred continuation beneath Quaternary deposits of the northwest-striking Clemens Well fault (Jennings, 1967; Powell, 1993). Sinistral strike slip on the Chiriaco and Salton Creek faults has been estimated as 11 km and as much as 14 km, respectively (see reviews by Powell, 1993, p. 59; Richard, 1993).

Powell (1993, p. 33) bracketed movement on his proposed Clemens Well–Fenner–San Francisquito fault as occurring between 22–20 Ma and 13 Ma, and possibly in the more restricted time interval between 18–17 Ma and 13 Ma. No middle Miocene units have been recorded in the vicinity of the Clemens Well segment of the fault, and the fault is not overlapped by any units older than Quaternary or possibly Pliocene. Both the northwestern projection of the Clemens Well fault and the western projection of the Chiriaco fault are buried beneath the Pleistocene Ocotillo fanglomerate in the Mecca Hills, and the Clemens Well fault may also locally be buried beneath upper Pliocene strata in this area (Powell, 1993). Similarly, the southern part of the Clemens Well fault is also covered by unfaulted, deeply incised fanglomerate of probable Pliocene or Pleistocene age (Powell, 1993). Movement may have continued until more recently on the Salton Creek fault, because crystalline rocks in the Chocolate Mountains south of the fault are locally faulted against Pliocene(?) or Pleistocene(?) fanglomerate north of the fault (Powell, 1993, p. 61).

Inversion Structures and Inferred Compression Directions

Folds

In the southern part of the Diligencia basin, the sedimentary fill has been deformed into a series of faulted folds (Figs. 3 and 4). These structures are dominated by a train of three large folds, two synclines separated by an anticline, and numerous associated minor folds. Field observations indicate that, away from the Clemens Well fault, folding of the Diligencia basin strata is approximately cylindrical. The three major folds are oriented approximately parallel to the long axis of the basin, and become progressively tighter and of greater amplitude traced from north to south. An analysis of the southernmost syncline-anticline pair is shown in Figure 11. For each fold, a least-squares method was used to construct a best-fit great circle through the maxima of poles to bedding. The inferred axis for each fold plunges gently west-northwest. In addition, the angle within the fold profile plane between the contoured maxima represents the average interlimb angle of each fold (87° and 84°, respectively, for the anticline and syncline). These analyses support the field observations that the folds are approximately parallel and that the interlimb angle decreases (albeit only modestly) from north to south.

Data related to fold orientation were also analyzed by recording trends of fold-hinge traces for all map-scale folds in the Diligencia Formation. In cases where the trend of a fold hinge is arcuate, multiple measurements were made in an attempt to avoid averaging out significant data during collection. Azimuthal data of fold-hinge trace trends were plotted on rose diagrams (Fig. 12). The data are sorted into two groups, those from the western part of the basin, and those from the eastern part of the basin. This separation was suggested by the observation that lineaments on the map appear to curve into the Clemens Well fault as they approach its outcrop position (cf. Figs. 3 and 12). The vector mean orientation of fold-hinge traces in the western part of the outcrop belt is ~20° different from the mean trend in the eastern part (Fig. 12). If this difference in orientation is the result of rotation of passive linear markers into the Clemens Well fault, then the folds in the eastern part of the basin (away from the fault zone) should give a more satisfactory estimate of the basin-scale maximum horizontal contraction direction than folds in the western part of the basin. The direction of maximum contraction inferred from the eastern portion of the area, and taken to be per-

pendicular to the mean fold-hinge trend, is 012° (Fig. 12).

Faults

Two broad categories of faults cut across the strata of the Diligencia Formation. The largest well-exposed faults in the area are long, northeast-striking, sigmoidal strike-slip faults in the eastern half of the basin (Fig. 3). These faults are remarkable in that the magnitude of displacement across them abruptly decreases laterally, from a maximum near the middle part of the fault, to zero at their ends. In the absence of common termination structures, these structures are interpreted as tear faults. If this interpretation is correct, then the faulting must have developed synchronously with folding of the basin fill.

The second category of faults in the Diligencia basin consists of numerous short, dextral and sinistral strike-slip and oblique-slip faults. In general, these faults strike either northeast or northwest. Whereas exceptions occur, those faults that strike northeast are commonly dextral, and those that strike northwest are commonly sinistral, based on observed offset of markers. As originally suggested by Powell (1981), the arrangement of faults is suggestive of a conjugate pair of fault sets, and this relationship is explored in Figure 13. Data were separated into two groups, those from the southern and western parts of the basin (Fig. 13A), and those from the northern and eastern parts of the basin farthest from the Clemens Well fault (Fig. 13, B and C).

The strikes of the faults in the southern and western parts of the basin cluster into one relatively tight grouping, with a vector mean trend of $\sim 057^\circ$ (Fig. 13A). Fault strikes from the northern and eastern parts of the basin form a diffuse spread (Fig. 13B); however, statistical tests indicate that this distribution is $<95\%$ likely to have been drawn from a random distribution. If the faults are separated by sense of offset into dextral and sinistral fault sets, they segregate into one tight cluster with a vector mean of 151° , and one diffuse cluster with a vector mean of 046° (Fig. 13C). Elementary stress theory predicts that the maximum principal compressive stress axis will bisect the acute angle between conjugate faults (Anderson, 1951). If these two populations of faults are considered a conjugate set, then the inferred maximum stress direction trends 009° . This is only 3° from the maximum contraction direction inferred from fold-hinge orientation in the eastern part of the basin (Fig. 12). The difference in orientation between faults in the southern and western (Fig. 13A) and north and eastern parts of the basin (Fig.

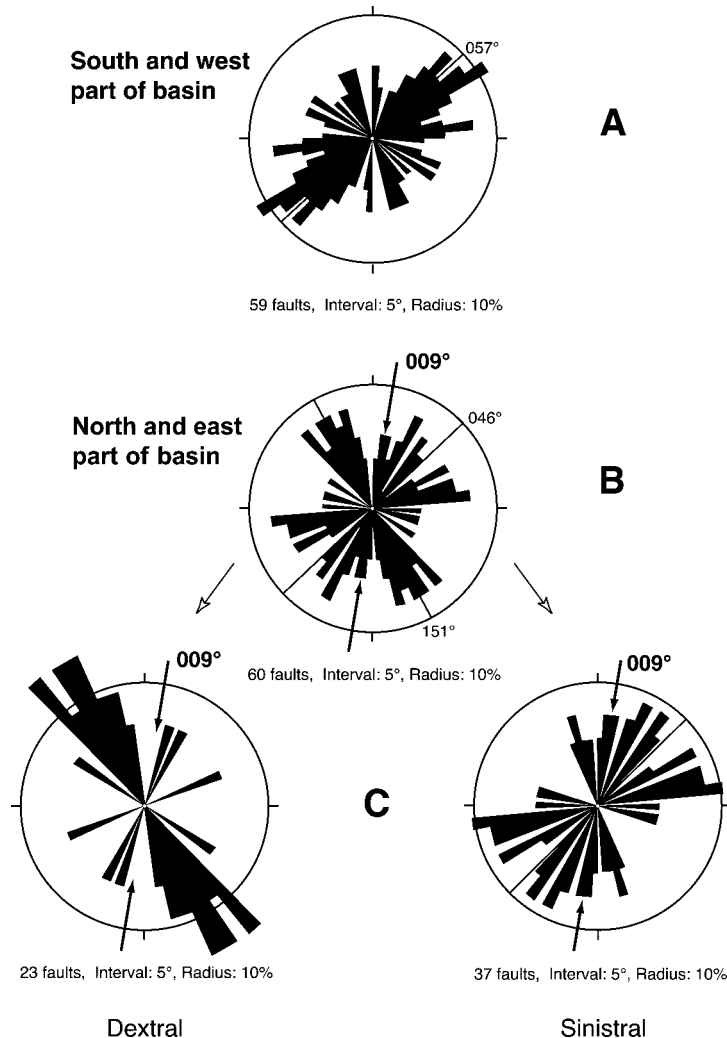


Figure 13. Circular histogram plots of minor fault trace strikes from the southern and western (A), and northern and eastern (B) parts of the Diligencia basin. Circular plots in (C) depict the same set of fault orientations as presented in (B), but divided into two groups by apparent sense of offset. The sense of offset was determined from field observations where available, and from map pattern where necessary; the direction of maximum principal compressive stress (represented by arrows) is inferred to bisect angle between the mean orientations of dextral (046°) and sinistral (151°) faults. See text for discussion.

13B) suggests that faults closer to the Clemens Well fault may have been rotated clockwise into the fault zone.

Extension Fractures

Data were selectively collected from barren and calcite-filled fractures within the Diligencia Formation that lack evidence of significant shearing. Poles to these planes exhibit two strong maxima with an acute intersection angle of 73° (Fig. 14A). The modal orientation of the strike of fractures is $\sim 010^\circ$ (Fig. 14B). These fractures are considered to represent extension cracks, rather than shear fractures, and

several examples were observed to be filled with concentrically zoned calcite layers, which lacked evidence of shearing. Extension fractures form by dilation in the direction of the least principal compressive stress and therefore are at least initially oriented parallel to the plane containing the other two principal stress axes. The 010° modal strike of the extension fractures across the Diligencia basin is nearly parallel to the maximum principal compressive stress direction inferred from both fold-axis trends (Fig. 12) and minor faults (Fig. 13B) in the eastern part of the basin away from the Clemens Well fault. These frac-

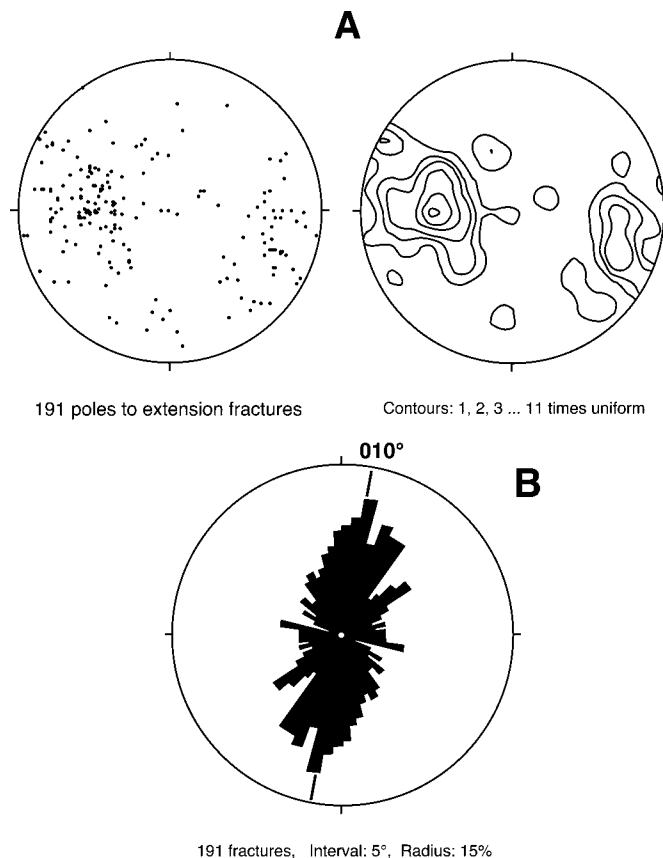


Figure 14. Structural analysis of extension fractures from the Diligencia Formation. (A) Poles to extension fractures plotted on equal-area net using the computer program Stereonet (Mancktelow, 1989). (B) Circular histogram plot of strike of extension fractures. Inferred direction of maximum principal compressive stress (010°) is taken to be parallel to the vector mean of strike and is shown by heavy line.

tures are also subparallel to calcite-filled extension fractures locally recorded by Davisson (1993) in sand and gravel of assumed Pliocene age (see following).

Data Synthesis and Correlation with Regional Studies

The fold, fault, and extension fracture data from the northern and eastern sections of the Diligencia basin imply remarkably consistent estimates for orientation of the maximum horizontal compression direction associated with basin inversion (009° – 012°). This compression direction is also consistent with both the generally accepted dextral sense of strike slip on the Clemens Well fault, and the observed 20° clockwise rotation of fold hinges adjacent to the fault (Figs. 3 and 12). If the fold, fault, and extension fracture data are plotted with respect to the Clemens Well fault, they compare favorably with ideal orientations predicted from clay-cake modeling studies of right-

slip faulting, such as those described by Harding (1974), although the Diligencia basin structures have formed at a consistently smaller angle to the main fault than those in the experimental data set (Fig. 15). Whether the Clemens Well fault initially formed, or was simply reactivated, as a right-slip fault during basin inversion remains uncertain. The observed 20° clockwise rotation of fold hinges adjacent to the fault indicates a dextral translation of 5–10 km parallel to the fault surface, using the graphical solutions for simple shear deformation by Ramsay (1967, p. 87), and assuming homogeneous simple shear over a 5-km-wide zone adjacent to the fault. A pure shear (transpressional) component across the fault zone would reduce the estimated displacement.

Inversion of the Diligencia basin could be simply a local transpressional phenomenon associated with strike slip on adjacent faults such as the Clemens Well and possibly the Salton Creek faults (see reviews by Sylvester,

1988; Lowell, 1995; Nilsen and Sylvester, 1995). However, the 009° – 012° trending maximum horizontal compression direction calculated for the Diligencia basin is very similar to the north-south contraction direction suggested by Bartley et al. (1990) to be associated with widespread folding and thrust faulting that postdates extension in the Mojave block north and east of the Diligencia basin. This suggests that inversion of the Diligencia basin may have occurred in response to regional compression, rather than localized transpressional deformation. Glazner et al. (2000) described inversion structures associated with north-south compression of a Miocene age basin in the Rodman Mountains (located 150 km north-northwest of the Diligencia basin; Fig. 2) that are remarkably similar to those we have described from the Diligencia basin. Both basins are elongate in an east-west direction and bounded to the west by northwest-striking right-slip faults and to the south by east-west-striking faults. Both basins contain gently dipping Miocene strata on their northern margins, and steeply dipping or overturned strata on their southern margins. In both basins the strata are folded about east-west-trending fold hinges that have been rotated in a clockwise direction traced westward toward the basin-bounding right-slip faults. These similarities suggest that similar mechanisms may be responsible for the development and inversion of both basins.

Regional-scale north-south contraction may have begun as early as 19 Ma in the Cady and Newberry Mountains (Fig. 2), and local folding in parts of the Mojave block of alluvial deposits of inferred Quaternary age suggests that contraction could be continuing at the present time (Bartley et al., 1990). Tectonic studies have consistently indicated that the entire lithosphere of the Mojave block has been in contraction for the past several million years (e.g., Bird and Rosenstock, 1985; Shufels and McNutt, 1986; Humphreys and Hager, 1990; Glazner and Bartley, 1994). Maximum horizontal stress orientations ($SH_{max} > S_v > SH_{min}$), inferred from azimuths of P axes for earthquake focal mechanisms associated with strike-slip faulting, trend between 007° and 020° in an ~ 100 km² area surrounding the Diligencia basin (Fig. 16), and traced to the northwest change to a north-south orientation associated with a component of thrust faulting in the Big Bend region of the San Andreas fault (Zoback et al., 1991; see also Stein et al., 1992; Shen-Tu et al., 1998, and references therein). Principal horizontal strain rate directions for shortening derived from Quaternary fault slip rates and recent geodetic

data (Shen-Tu and Holt, 1999) are subparallel to the maximum horizontal stress orientations in this region. Close to the Diligencia basin, present-day maximum horizontal stress orientations inferred from focal mechanisms for one seismic event trend 009° (Fig. 16), i.e., subparallel to the maximum compression direction (009° – 012°) inferred from inversion structures in the basin (Figs. 12–15).

Timing of Basin Inversion and Block Rotation

Precise dating of inversion and block rotation for the Diligencia basin is problematic. The K-Ar dating of the youngest basalt flows within the Diligencia Formation has yielded an age of 21.3 ± 0.6 Ma (Frizzell and Weigand, 1993), but no precise upper age limit can be assigned to the folded and faulted strata because of the lack of diagnostic fossils or fresh volcanic rocks in the upper part of the section (Spittler and Arthur, 1982). A provisional age of 16 Ma was ascribed by J.C. Crowell (*in* Sherrod and Nielson, 1993, Plate 3) to the youngest preserved rocks of the Diligencia Formation. On the east and northeast sides of the basin, these deformed strata are unconformably overlain by flat-lying Pliocene–Pleistocene terrace gravels (Spittler and Arthur 1982, p. 85), indicating an upper age limit for inversion. The oldest deposits include relatively rare conglomeratic sands, which may be the lateral equivalents of either the Miocene Mecca Formation or the Pliocene(?)–Pleistocene Palm Spring Formation recorded to the northwest of the Diligencia basin (Sylvester and Smith, 1975, 1976). Locally the oldest deposits are cut by calcite-filled extension fractures; these fractures also cut across the underlying Diligencia Formation strata, but do not affect younger strata, which may be correlated with the Pleistocene Ocotillo Formation (Davisson, 1993). These data bracket inversion of the Diligencia basin between ca. 16 Ma and 2 Ma.

Data discussed herein indicate that inversion was associated with a phase of north-south-directed contraction; this phase is also recognized in the Mojave block north of the Diligencia basin (e.g., Bartley et al., 1990; Glazner et al., 2000). Bartley et al. (1990) demonstrated that this contraction may have begun as early as 19 Ma in the Cady and Newberry Mountains (Fig. 2), but earthquake data (Fig. 16) indicate that north-south compression may still be occurring in the Orocopia Mountains adjacent to the Diligencia basin (Zoback et al., 1991). It is important to note that the evidence for early north-south com-

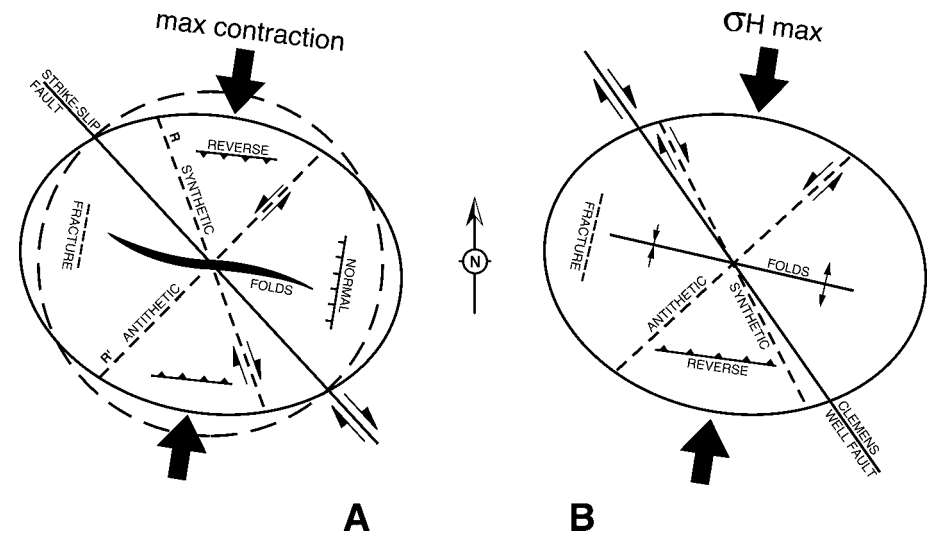


Figure 15. Schematic diagrams of strain ellipse and idealized fold and fault orientations associated with a 010° – 190° contraction direction. (A) Comparison of ideal average orientations of minor structures with respect to a major right-slip fault (adapted from Sylvester and Smith, 1976); note that only very low penetrative finite strain and minimal rotation of structures are assumed. (B) Comparison of the average orientation of inversion structures in the eastern part of the Diligencia basin (see also Figs. 3 and 12–14) with the average orientation of the Clemens Well fault.

pression (in present-day coordinates) comes from parts of the Mojave block that apparently have not been subjected to Neogene block rotation (see summary map by Dickinson, 1996, p. 16).

In contrast, paleomagnetic data indicate that the Diligencia basin has undergone large-magnitude apparent rotation. The close similarity between (1) the 010° contraction direction inferred from the folds, faults, and extension fractures that affect the Diligencia Formation, (2) the north-south contraction recognized in the unrotated sections of the Mojave block to the north, and (3) the present-day 009° compression direction indicated by earthquake data close to the Diligencia basin (all in present-day coordinates) strongly indicate that rotation of the crustal block containing the Diligencia basin occurred before basin inversion. The only alternative explanation is that if inversion began before rotation had ceased, then the Diligencia basin structures have been fortuitously rotated into an orientation currently indicative of north-south contraction. As outlined here, precise timing of the onset and cessation of strike-slip faulting and associated block rotation in the Mojave Desert region remains uncertain. Luyendyk (1991) suggested that clockwise block rotation of the eastern Transverse Ranges may have begun ca. 6.5 Ma and is continuing now, while Richard (1993) regarded rotation as being bracketed between 10 ± 2 Ma and $4.5 \pm$

0.2 Ma. Our data from the Diligencia basin are compatible with the time frame proposed by Richard (1993) for block rotation, and this would imply a latest Miocene to Pliocene age for basin inversion if his younger time limit for rotation is assumed.

Speculative Tectonic Model for Basin Inversion

Given a regional north-south compression, we speculate that internal deformation of the elongate crustal block containing the Diligencia basin and bounded by the currently north-west-striking San Andreas (or Clemens Well) and Sheep Hole faults and the east-west-striking Chiriaco and Salton Wash faults (Fig. 2) began when the block reached an east-west orientation, and was unable to continue accommodating regional scale north-south shortening by rigid-body rotation (*cf.* Nur et al., 1993). In this speculative model, basin inversion is therefore ultimately the result of the locking, and subsequent internal deformation, of a previously passively rotating elongate crustal block within a continuing regional scale compressive stress field.

This model does not exclude the possibility that dextral shearing on the Clemens Well fault (either related or unrelated to rotation of crustal blocks) may have occurred before, during and, at least in a minor sense, after the main stages of basin inversion. As discussed

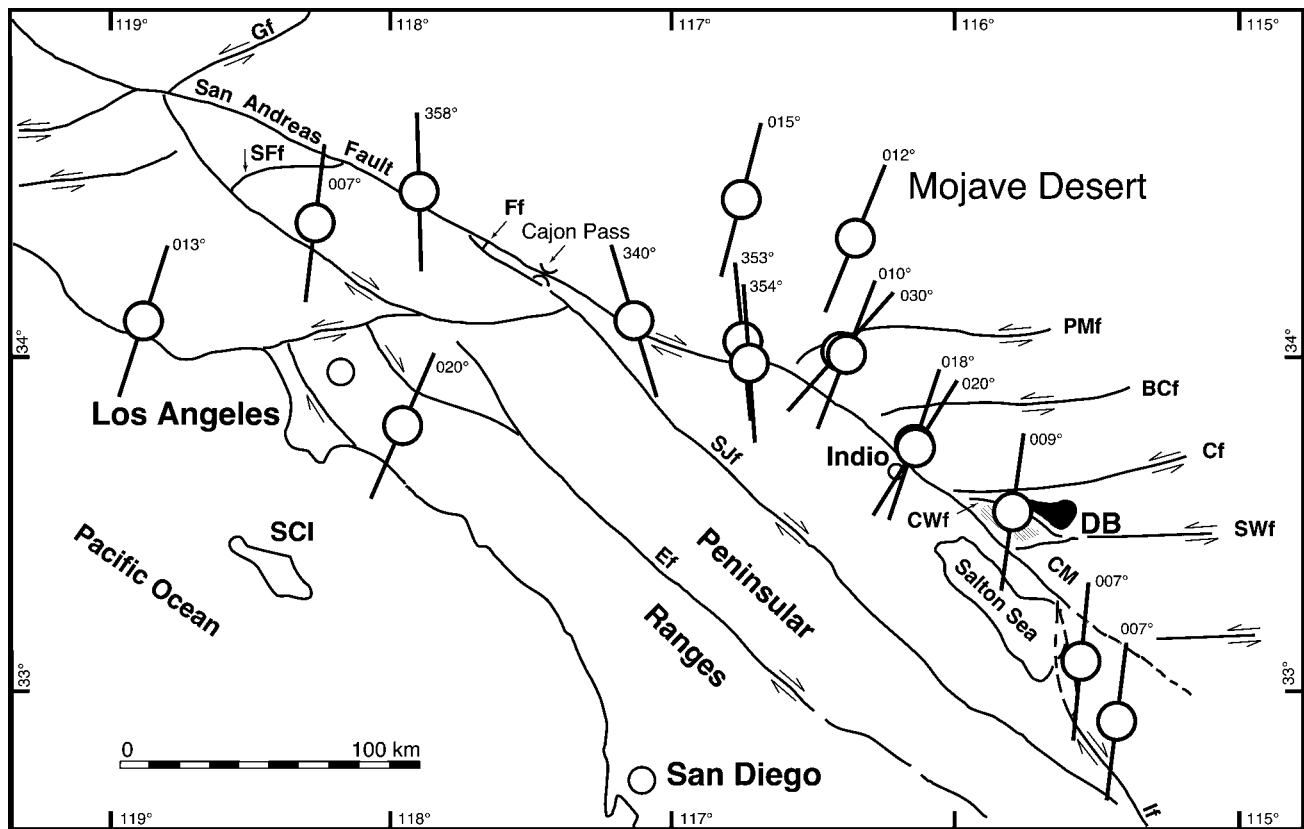


Figure 16. Maximum horizontal stress orientations ($SH_{max} > S_v > SH_{min}$) inferred from azimuths of P axes for earthquake focal mechanisms associated with strike slip faulting (adapted from Zoback et al., 1991). Close to the Diligencia basin, present-day maximum horizontal stress orientation inferred from focal mechanisms for one seismic event trends 009° , i.e., subparallel to the maximum compression direction (009° – 012°) inferred from inversion structures in the basin (Figs. 12–15). See Figure 2 for explanation of abbreviations used.

herein, fold hinges associated with basin inversion are rotated clockwise toward parallelism with the adjacent Clemens Well fault (Figs. 2 and 12), indicating that shearing along the fault either accompanied or postdated inversion. Motion on the Clemens Well fault appears to have ceased, however, before late Pliocene time (Powell, 1993). Terres (1984) argued that clockwise rotation of the Diligencia Formation strata against the Clemens Well fault must have begun before initiation of folding (i.e., inversion), because the local change in paleomagnetic declination toward the fault is more than five times greater than the rotation indicated by change in fold-hinge orientation. Modeling of rotating crustal blocks (Nilsen and Sylvester, 1995, their Fig. 12.3.c) indicates that transpression would have begun in the southwest corner of this clockwise-rotating block (i.e., on the section of the Clemens Well fault adjacent to the Diligencia basin) at an early stage of rigid-body rotation. This model may offer an explanation for the large apparent clockwise rotation in-

indicated by paleomagnetic declination anomalies in the Diligencia Formation, relative to the surrounding regions.

CONCLUSIONS

1. Facies analyses indicate that latest Oligocene and lower Miocene (ca. 24–16 Ma) fluvial and volcanic rocks of the Diligencia Formation were deposited in a half-graben with (in present-day coordinates) a steep, possibly fault-controlled, south-facing northern escarpment, and a more gentle north-facing southern slope. Paleocurrent data, particularly from the high-energy deposits on the northern basin margin, indicate stream flow toward the southeast and south-southeast, oblique to the mapped east-west-trending basin margins, and suggest an approximate northeast to east-northeast trend for the Diligencia basin.

2. Previously published paleomagnetic data indicate that rocks of the Diligencia basin may have been rotated clockwise by no more than 110° about a vertical axis since deposition

ceased. If correct, this would suggest that the basin originally opened to between the east-northeast and northeast, subparallel to well-documented extension directions in Miocene age basins in the Mojave Desert to the north and east. Initial formation of the basin in latest Oligocene to lowermost Miocene times, however, may have predated the main phase of Basin and Range extension by 1–2 m.y.

3. Previously published palinspastic restorations have proposed that the Diligencia basin was originally contiguous with the Oligocene–Miocene age Soledad and Plush Ranch basins, now located 250–320 km to the northwest on the opposite (west) side of the San Andreas fault. However, facies analyses coupled with paleomagnetic data indicate that the Plush Ranch and Soledad basins originally opened to the north and northwest, respectively, thereby bringing into question the proposed juxtaposition of these basins.

4. Rocks of the Diligencia basin are locally intensely folded and faulted but are unconformably overlain by flat-lying latest Plio-

cene(?) and Pleistocene strata. Kinematic analysis of the folds, conjugate strike-slip faults, and extension fractures indicates that basin inversion was associated with north-south horizontal contraction. Inversion could be simply a local transpressional phenomenon associated with strike slip on adjacent faults. However, the 009°–012° trending maximum horizontal compression direction calculated for the structures associated with basin inversion is sub-parallel to both the north-south contraction direction inferred from tectonic structures cutting Miocene strata in unrotated sections of the Mojave block to the north and the present-day compression directions indicated by earthquake data adjacent to the Diligencia basin. This parallelism suggests that basin inversion was associated with regional-scale, and ongoing, north-south compression.

5. The Diligencia basin is situated in an elongate, currently east-west-trending fault block bounded to the west by the San Andreas fault. Clockwise rotation on east-west fault blocks in this region (45°–110° depending on data and model used) is bracketed between ca. 10 and 4.5 Ma. Structural and paleomagnetic data indicate that basin inversion occurred after block rotation, implying a latest Miocene to Pliocene age for inversion. We speculate that basin inversion, within a north-south compressive stress field, resulted from the locking and subsequent internal deformation of this previously passively rotating elongate crustal block.

ACKNOWLEDGMENTS

Field work was funded by National Science Foundation grant EAR-9018929 to Law, and student grants from the Geological Society of America to C.M. Davison. We thank John Crowell, Julia Miller, Art Sylvester, and Associate Editor Doug Walker for reviewing different versions of the manuscript, and John Bartley, Allen Glazner, Ray Ingersoll, and Jim Spotila for discussions. We particularly thank John Crowell for suggesting important organizational changes to the manuscript, which led to placing our study in a broader regional context.

REFERENCES CITED

- Anderson, E.M., 1951, The dynamics of faulting: Edinburgh, Oliver and Boyd, 206 p.
- Arthur, M.A., 1974, Stratigraphy and sedimentation of lower Miocene non-marine strata of the Orocochia Mountains; constraints for late Tertiary slip on the San Andreas fault system in southern California [M.S. thesis]: Riverside, University of California, 200 p.
- Atwater, T.M., 1970, Implications of plate tectonics for the Cenozoic tectonic evolution of western North America: Geological Society of America Bulletin, v. 81, p. 3513–3536.
- Atwater, T.M., and Stock, J., 1998, Pacific–North America plate tectonics of the Neogene southwestern United States: An update, in Ernst, W.G., and Nelson, C.A., eds., Integrated Earth and environmental evolution of the southwestern United States. The Clarence A. Hall, Jr. Volume: Columbia, Maryland, Bellwether Publishing for Geological Society of America, p. 393–420.
- Axelrod, D.I., 1950, Studies in Late Tertiary paleobotany: Contributions to Paleontology: Washington, D.C., Carnegie Institution of Washington, 323 p.
- Axen, G.J., and Fletcher, J.M., 1998, Late Miocene–Pleistocene extensional faulting, northern Gulf of California, Mexico and Salton Trough, California, in Ernst, W.G., and Nelson, C.A., eds., Integrated Earth and environmental evolution of the southwestern United States. The Clarence A. Hall, Jr. Volume: Columbia, Maryland, Bellwether Publishing for Geological Society of America, p. 365–392.
- Baker, E.D., Buckner, G.T., and Frost, E.G., 1991, Regional detachment faulting in west-central California and its offset from and comparison to crustal extension in the SE California detachment terrane: Geological Society of America Abstracts with Programs, v. 23, no. 5, p. A132.
- Bartley, J.M., and Glazner, A.F., 1991, En echelon Miocene rifting in the southwestern United States and model for vertical-axis rotation in continental extension: Geology, v. 19, p. 1165–1168.
- Bartley, J.M., Glazner, A.F., and Schermer, E.R., 1990, North-south contraction of the Mojave Block and strike-slip tectonics in southern California: Science, v. 248, p. 1398–1401.
- Bartow, J.A., 1990, Coarse-grained deltaic sedimentation in the Miocene Cuyama strike slip basin, California Coast Ranges: Sedimentary Geology, v. 68, p. 17–38.
- Beatty, C.B., 1990, Anatomy of a White Mountains debris flow—The making of an alluvial fan, in Rachocki, A.H., and Church, M., eds., Alluvial fans: A field approach: Chichester, John Wiley, p. 68–89.
- Best, M.G., 1988, Early Miocene change in direction of least principal stress, southwestern United States: Conflicting inferences from dikes and metamorphic core–detachment-fault terranes: Tectonics, v. 7, p. 249–259.
- Bird, P., and Rosenstock, R.W., 1984, Kinematics of present crust and mantle flow in southern California: Geological Society of America Bulletin, v. 95, p. 946–957.
- Bishop, K.M., and Ehlig, P.L., 1990, The Pelona fault, Central Transverse Ranges, southern California: An extensional detachment fault?: Geological Society of America Abstracts with Programs, v. 22, no. 3, p. 8.
- Blake, M.C., Campbell, R.H., Dibblee, T.W., Jr., Howel, D.G., Nilsen, T.H., Normark, W.R., Vedder, J.C., and Silver, E.A., 1978, Neogene basin formation in relation to plate-tectonic evolution of the San Andreas Fault system, California: American Association of Petroleum Geologists Bulletin, v. 62, p. 344–372.
- Blythe, A.E., Burbank, D.W., Farley, K.A., and Fielding, E.J., 2000, Structural and topographic evolution of the central Transverse Ranges, California, from apatite fission-track, (U-Th)/He and digital elevation model analysis: Basin Research v. 12, p. 97–114.
- Bohannon, R.G., 1975, Mid-Tertiary conglomerates and their bearing on Transverse Range tectonics, southern California: California Division of Mines and Geology Special Report 118, p. 75–82.
- Bohannon, R.G., and Geist, E., 1998, Upper crustal structure and Neogene tectonic development of the California continental borderland: Geological Society of America Bulletin, v. 110, p. 779–800.
- Bohannon, R.G., and Parsons, T., 1995, Tectonic implications of post-30 Ma Pacific and North American relative plate motions: Geological Society of America Bulletin, v. 107, p. 937–959.
- Boothroyd, J.C., and Ashley, G.M., 1975, Processes, bar morphology, and sedimentary structures on braided outwash fans, northeastern Gulf of Alaska, in Jopling, A.V., and McDonald, B.C., eds., Glaciofluvial and glaciolacustrine sedimentation: Society of Economic Paleontologists and Mineralogists Special Publication 23, p. 193–222.
- Buckner, G.T., Baker, E.D., and Frost, E.G., 1991, Mid-Tertiary detachment faulting in the Cuyama Basin and Lockwood Valley area, southern California: Geological Society of America Abstracts with Programs, v. 23, no. 5, p. A131–132.
- Buchanan, J.G., and Buchanan, P.G., eds., 1995, Basin inversion: Geological Society [London] Special Publication 88, 596 p.
- Burchfiel, B.C., and Davis, G.A., 1981, Mojave desert and environs, in Ernst, W.G., ed., The geotectonic development of California: Rubey Volume 1: Englewood Cliffs, New Jersey, Prentice-Hall, p. 217–252.
- Carter, N.J., Luyendyk, B.P., and Terres, R.R., 1987, Neogene clockwise rotation of Eastern Transverse Ranges, California, suggested by paleomagnetic vectors: Geological Society of America Bulletin, v. 98, p. 199–206.
- Cole, R.B., and Stanley, R.G., 1995, Middle Tertiary extension recorded by lacustrine fan-delta deposits, Plush Ranch basin, Western Transverse Ranges, California: Journal of Sedimentary Research, v. B65, p. 455–468.
- Cooper, M.A., and Williams, G.D., eds., 1989, Inversion tectonics: Geological Society [London] Special Publication 44, 375 p.
- Cox, A., 1980, Rotation of microplates in western North America, in Strangway, D.W., ed., The continental crust and its mineral deposits: Geological Association of Canada Special Paper 20, p. 305–321.
- Crouch, J.K., and Suppe, J., 1993, Late Cenozoic tectonic evolution of the Los Angeles basin and inner California borderland: A model for core complex-like crustal extension: Geological Society of America Bulletin, v. 105, p. 1415–1434.
- Crowell, J.C., 1960, The San Andreas fault in southern California: International Geological Congress, 21, Report, Part 18, p. 45–63.
- Crowell, J.C., 1962, Displacement along the San Andreas fault, California: Geological Society of America Special Paper 71, 61 p.
- Crowell, J.C., 1968, Movement histories of faults in the Transverse Ranges and speculations on the tectonic history of California, in Dickinson, W.R., and Grantz, A., eds., Proceedings of the conference on geologic problems of San Andreas fault system: Stanford University Publications in the Geological Sciences, v. 11, p. 323–341.
- Crowell, J.C., 1973, Problems concerning the San Andreas fault system in southeastern California: Stanford University Publications in the Geological Sciences, v. 13, p. 125–135.
- Crowell, J.C., 1974a, Origin of late Cenozoic basins in southern California, in Dickinson, W.R., ed., Tectonics and sedimentation: Society of Economic Paleontologists and Mineralogists Paper 38, p. 190–204.
- Crowell, J.C., 1974b, The Orocochia thrust, southeastern California: Geological Society of America Abstracts with Programs, v. 6, p. 159.
- Crowell, J.C., 1975, Geologic sketch of the Orocochia Mountains, southeastern California, in Crowell, J.C., ed., San Andreas fault in southern California: A guide to the San Andreas fault from Mexico to Carrizo Plain: California Division of Mines and Geology Special Report 118, p. 99–110.
- Crowell, J.C., 1981, An outline of the tectonic history of southeastern California, in Ernst, W.G., ed., The geotectonic development of California: Rubey Volume 1: Englewood Cliffs, New Jersey, Prentice-Hall, p. 584–599.
- Crowell, J.C., 1982, The tectonics of the Ridge basin, southern California, in Crowell, J.C., and Link, M.H., eds., Geologic history of Ridge basin, southern California: Los Angeles, California, Pacific Section, Society of Economic Paleontologists and Mineralogists, p. 25–42.
- Crowell, J.C., 1987, Late Cenozoic basins of onshore southern California: Complexity is the hallmark of their sediment character, in Ingersoll, R.V., and Ernst, W.G., eds., Cenozoic basin development of coastal California: Rubey Volume 6: Englewood Cliffs, New Jersey, Prentice-Hall, p. 207–241.
- Crowell, J.C., 1993a, Introduction to Tertiary rocks of the far-west basins, in Sherrod, D.R., and Nielsen, J.E., eds., Tertiary stratigraphy of highly extended terranes, California, Arizona, and Nevada: U.S. Geological Survey Bulletin 2053, p. 235–238.
- Crowell, J.C., 1993b, The Diligencia Formation, Orocochia Mountains, southeastern California, in Sherrod, D.R., and Nielsen, J.E., eds., Tertiary stratigraphy of highly

- extended terranes, California, Arizona, and Nevada: U.S. Geological Survey Bulletin 2053, p. 239–242.
- Crowell, J.C., and Link, M.H., 1982, Geologic history of Ridge basin, southern California: Los Angeles, California, Pacific Section, Society of Economic Paleontologists and Mineralogists, 304 p.
- Crowell, J.C., and Susuki, T., 1959, Eocene stratigraphy and paleontology, Orocochia Mountains, southern California: Geological Society of America Bulletin, v. 70, p. 581–592.
- Crowell, J.C., and Walker, J.W.R., 1962, Anorthosite and related rocks along the San Andreas fault, southern California: University of California Publications in Geological Sciences, v. 40, p. 219–288.
- Cummings, D., Weiss, J., and Haines, E.L., 1982, Cretaceous and Miocene fission-track retention ages from Precambrian rocks, and thermal history of the western San Gabriel Mountains, southern California, in Fife, D.L., and Minch, J.A., eds., Geology and mineral wealth of the California Transverse Ranges: Santa Ana, California, South Coast Geological Society, p. 297–303.
- Davissson, C.M., 1993, Stratigraphic and structural evolution of the early Diligencia basin, Orocochia Mountains, southeastern California [M.S. thesis]: Blacksburg, Virginia Polytechnic Institute and State University, 142 p.
- DeCelles, P.G., 1988, Middle Cenozoic depositional, tectonic and sea level history of the southern San Joaquin basin, California: American Association of Petroleum Geologists Bulletin, v. 72, p. 1297–1322.
- DeLuca, J.L., and Eriksson, K.A., 1989, Controls on synchronous ephemeral and perennial-river sedimentation in the middle sandstone member of the Triassic Chinle Formation, N.E. New Mexico: Sedimentary Geology, v. 61, p. 155–175.
- Dickinson, W.R., 1996, Kinematics of transrotational tectonism in the California Transverse Ranges and its contribution to cumulative slip along the San Andreas transform fault system: Geological Society of America Special Paper 305, 46 p.
- Dickinson, W.R., 1997, Tectonic implications of Cenozoic volcanism in coastal California: Geological Society of America Bulletin, v. 109, p. 936–954.
- Dillon, J.T., 1975, Geology of the Chocolate and Cargo Muchacho Mountains, southeasternmost California [Ph.D. thesis]: Santa Barbara, University of California, 380 p.
- Dillon, J.T., and Ehlig, P.L., 1993, Displacement on the southern San Andreas fault, in Powell, R.E., et al., eds., The San Andreas fault system: Displacement, palinspastic reconstruction and geologic evolution: Geological Society of America Memoir 178, p. 199–216.
- Dillon, J.T., Haxel, G.B., and Tosdal, R.M., 1990, Structural evidence for northeastward movement on the Chocolate Mountains thrust, southeasternmost California: Journal of Geophysical Research, v. 95, p. 19953–19971.
- Dokka, R.K., and Ross, T.M., 1995, Collapse of southwestern North America and the evolution of early Miocene detachment faults, metamorphic core complexes, the Sierra Nevada orocline, and the San Andreas fault system: Geology, v. 23, p. 1075–1078.
- Dokka, R.K., and Travis, C.J., 1990a, Late Cenozoic strike-slip faulting in the Mojave Desert, California: Tectonics, v. 9, p. 311–340.
- Dokka, R.K., and Travis, C.J., 1990b, Role of the eastern California shear zone in accommodating Pacific–North American plate motion: Geophysical Research Letters, v. 17, p. 1323–1326.
- Dokka, R.K., Henry, D.J., Ross, T.M., Baksi, A.K., Lambert, J., Travis, C.J., Jones, S.M., Jacobson, C., McCurdy, M.M., Woodburne, M.O., and Ford, J.P., 1991, Aspects of the Mesozoic and Cenozoic geologic evolution of the Mojave Desert, in Walamender, M.J., and Hanan, B.B., eds., Geologic excursions in southern California and Mexico (Geological Society of America Annual Meeting Guidebook): San Diego, California, San Diego State University, Department of Geological Sciences, p. 1–43.
- Dokka, R.K., Ross, T.M., and Lu, G., 1998, The Trans Mojave-Sierran shear zone and its role in early Miocene collapse of southwestern North America, in Holdsworth, R.E., et al., eds., Continental transpressional and transtensional tectonics: Geological Society [London] Special Publication 135, p. 183–202.
- Dreyer, T., 1993, Quantified fluvial architecture in ephemeral stream deposits of the Esplugafreda Formation (Palaeocene), Tremp-Graus basin, northern Spain, in Marzo, M., and Puigdefabregas, C., eds., Alluvial sedimentation: International Association of Sedimentologists Special Publication 17, p. 337–362.
- Ehlert, K.W., 1982, Basin analysis of the Miocene Mint Canyon Formation, southern California, in Ingersoll, R.V., and Woodburne, M.O., eds., Cenozoic nonmarine deposits of California and Arizona: Pacific Section, Society of Economic Paleontologists and Mineralogists, p. 51–64.
- Ehlig, P.L., 1958, Geology of the Mount Baldy region of the San Gabriel Mountains, California [Ph.D. thesis]: Los Angeles, University of California, 192 p.
- Ehlig, P.L., 1968, Causes of distribution of Pelona, Rand and Orocochia Schist along the San Andreas and Garlock faults, in Dickinson, W.R., and Grantz, A., eds., Proceedings of the conference on geologic problems of San Andreas fault system: Stanford University Publications in the Geological Sciences, v. 11, p. 294–305.
- Ehlig, P.L., 1981, Origin and tectonic history of the basement terrane of the San Gabriel Mountains, Central Transverse Ranges, in Ernst, W.G., ed., The geotectonic development of California: Rubey Volume 1: Englewood Cliffs, New Jersey, Prentice-Hall, p. 254–283.
- Engel, A.E., and Schultejan, P.A., 1984, Late Mesozoic and Cenozoic tectonic history of south central California: Tectonics, v. 3, p. 659–675.
- Fatahipour, M., and Frost, E.G., 1991, Mid-Tertiary extensional development of the Los Angeles basin and its disruption of the Mesozoic accretionary wedge and convergent margin sequence (Catalina schist and Orocochia schist): Geological Society of America Abstracts with Programs, v. 23, no. 5, p. A132.
- Fatahipour, M., and Frost, E.G., 1996, Low-angle normal faulting along southern coastal California as displayed by the hanging-wall rollover geometry of the San Ofre breccia, in Abbott, P.L., and Cooper, J.D., eds., Field conference guidebook and volume for the American Association of Petroleum Geologists, Annual Convention, San Diego, California: Bakersfield, Pacific Section American Association of Petroleum Geologists Guidebook 73, p. 285–294.
- Fedo, C.M., and Miller, J.M.G., 1992, Evolution of a Miocene half-graben basin, Colorado River extensional corridor, southeastern California: Geological Society of America Bulletin, v. 104, p. 481–493.
- Fisher, R.V., 1971, Features of coarse-grained, high-concentration fluids and their deposits: Journal of Sedimentary Petrology, v. 41, p. 916–927.
- Frizzell, V.A., Jr., and Weigand, P.W., 1993, Whole-rock K-Ar ages and geochemical data from the middle Cenozoic volcanic rocks, southern California: A test of correlations across the San Andreas fault, in Powell, R.E., et al., eds., The San Andreas fault system: Displacement, palinspastic reconstruction and geologic evolution: Geological Society of America Memoir 178, p. 273–288.
- Frost, E.G., and Martin, D.L., 1983, Overprint of Tertiary detachment deformation on the Mesozoic Orocochia schist and Chocolate Mountain thrust: Geological Society of America Abstracts with Programs, v. 15, p. 577.
- Frost, E.G., Cameron, T.E., Krummenacher, D., and Martin, D., 1981, Possible regional interaction of mid-Tertiary detachment faulting with the San Andreas fault and the Vincent-Orocochia thrust system, Arizona and California: Geological Society of America Abstracts with Programs, v. 13, p. 455.
- Glazner, A.F., and Bartley, J.M., 1984, Timing and tectonic setting of Tertiary low-angle normal faulting and associated magmatism in the southwestern United States: Tectonics, v. 3, p. 385–396.
- Glazner, A.F., and Bartley, J.M., 1994, Eruption of alkali basalts during crustal shortening in southern California: Tectonics, v. 13, p. 493–498.
- Glazner, A.F., Bartley, J.M., and Sanner, W.K., 2000, Nature of the southwestern boundary of the central Mojave Tertiary province, Rodman Mountains, California: Geological Society of America Bulletin, v. 112, p. 34–44.
- Goodmacher, J., Barnett, L., Buckner, G., Ouchrif, L., Vidigal, A., and Frost, E., 1989, The Clemens Well fault in the Orocochia Mountains of southern California: A strike-slip or normal fault structure?: Geological Society of America Abstracts with Programs, v. 21, no. 5, p. 85.
- Goodman, E.D., and Malin, P.E., 1992, Evolution of the southern San Joaquin basin and mid-Tertiary “transitional” tectonics, central California: Tectonics, v. 11, p. 478–498.
- Graham, S.A., McCloy, C., Hitzman, M., Ward, R., and Turner, R., 1984, Basin evolution during change from convergent to transform continental margin in central California: American Association of Petroleum Geologists Bulletin, v. 68, p. 233–249.
- Graham, S.A., Stanley, G.B., Bent, J.V., and Carter, J.B., 1989, Oligocene and Miocene paleogeography of central California and displacement along the San Andreas fault: Geological Society of America Bulletin, v. 101, p. 711–730.
- Hamblin, A.P., and Rust, B.R., 1989, Tectono-sedimentary analysis of alternate polarity half-graben basin-fill successions: Late Devonian–Early Carboniferous Horton Group, Cape Breton Island, Nova Scotia: Basin Research, v. 2, p. 239–255.
- Hamilton, W., 1987, Mesozoic geology and tectonics of the Big Maria Mountains region, southeastern California, in Dickinson, W.R., and Klute, M.A., eds., Mesozoic rocks of southern Arizona and adjacent areas: Arizona Geological Society Digest, v. 18, p. 33–47.
- Hardie, L.A., and Eugster, H.P., 1970, The evolution of closed basin brines, in Morgan, B.A., ed., Mineralogy and geochemistry of nonmarine evaporites: Mineralogical Society of America Special Publication 3, p. 273–290.
- Hardie, L.A., Smoot, J.P., and Eugster, H.P., 1978, Saline lakes and their deposits: A sedimentological approach, in Matter, A., and Tucker, M.E., eds., Modern and ancient lake sediments: International Association of Sedimentologists Special Publication 2, p. 7–41.
- Harding, T.P., 1974, Petroleum traps associated with wrench faults: American Association of Petroleum Geologists Bulletin, v. 58, p. 1290–1304.
- Haxel, G., 1977, The Orocochia Schist and Vincent–Chocolate Mountain thrust in the Picacho-Peter Kane Mountain area, southeasternmost California [Ph.D. thesis]: Santa Barbara, University of California, 277 p.
- Haxel, G.B., and Dillon, J., 1978, The Pelona-Orocochia Schist and Vincent–Chocolate Mountain thrust system, southern California, in Howell, D.G., and McDougal, K.A., eds., Mesozoic paleogeography of the western United States: Pacific Section, Society of Economic Paleontologists and Mineralogists, Pacific Coast Paleogeography Symposium 2, p. 453–469.
- Haxel, G.B., and Tosdal, R.M., 1986, Significance of the Orocochia Schist and Chocolate Mountains thrust in the late Mesozoic tectonic evolution of the southeastern California–southwestern Arizona region [extended abs.]: Arizona Geological Society Digest, v. 16, p. 52–61.
- Haxel, G.B., Tosdal, R.M., and Dillon, J.T., 1985, Tectonic setting and lithology of the Winterhaven Formation: A new Mesozoic stratigraphic unit in southeasternmost California and southwestern Arizona: U.S. Geological Survey Bulletin 1599, 19 p.
- Haxel, G.B., Budahn, J.R., Fries, T.L., King, B.W., White, L.D., and Aruscavage, P.J., 1987, Geochemistry of the Orocochia Schist, southeastern California: Summary, in Dickinson, W.R., and Klute, M.A., eds., Mesozoic rocks of southern Arizona and adjacent areas: Arizona Geological Society Digest, v. 18, p. 49–64.
- Hendrix, E.P., 1993, Soledad basin, Central Transverse Ranges, California, in Sherrod, D.R., and Nielson, J.E., eds., Tertiary stratigraphy of highly extended terranes, California, Arizona, and Nevada: U.S. Geological Survey Bulletin 2053, p. 243–250.
- Hendrix, E.P., and Ingersoll, R.V., 1987, Tectonics and alluvial sedimentation of the upper Oligocene–lower Miocene Vasquez Formation, Soledad basin, southern

- California: Geological Society of America Bulletin, v. 98, p. 647–663.
- Hooke, R.L., 1967, Processes on arid-region alluvial fans: *Journal of Geology*, v. 75, p. 438–460.
- Hornafius, J.S., Luyendyk, B.P., Terres, R.R., and Kamerling, M.J., 1986, Timing and extent of Neogene tectonic rotation in the Western Transverse Ranges, California: Geological Society of America Bulletin, v. 97, p. 1476–1487.
- Howard, K.A., and Hopson, R.F., 1997, Vertical axis rotations in the Mojave: Evidence from the Independence dike swarm: Comment and reply: *Geology*, v. 25, p. 1051–1052.
- Hughes, K.M., 1993, The conglomerate of Bear Canyon (Miocene), Chocolate Mountains, southeastern California, in Sherrod, D.R., and Nielsen, J.E., eds., Tertiary stratigraphy of highly extended terranes, California, Arizona, and Nevada: U.S. Geological Survey Bulletin 2053, p. 213–216.
- Humphreys, E.D., and Hager, B.H., 1990, A kinematic model for the late Cenozoic development of southern California crust and mantle: *Journal of Geophysical Research*, v. 95, p. 19747–19762.
- Humphreys, E.D., and Weldon, R.J., II, 1994, Deformation across the western United States: A local estimate of Pacific-North America transform deformation: *Journal of Geophysical Research*, v. 99, p. 19975–20010.
- Jackson, J., and Molnar, P., 1990, Active faulting and block rotations in the western Transverse Ranges, California: *Journal of Geophysical Research*, v. 95, p. 22073–22087.
- Jacobson, C.E., 1990, The $^{40}\text{Ar}/^{39}\text{Ar}$ geochronology of the Pelona schist and related rocks, southern California: *Journal of Geophysical Research*, v. 95, p. 509–528.
- Jacobson, C.E., and Dawson, M.R., 1995, Structural and metamorphic evolution of the Orocoopia schist and related rocks, southern California: Evidence for late movement on the Orocoopia fault: *Tectonics*, v. 14, p. 933–944.
- Jacobson, C.E., Dawson, M.R., and Postlethwaite, C.E., 1987, Evidence for late-stage normal slip on the Orocoopia thrust and implications for the Vincent–Chocolate Mountains thrust problem: Geological Society of America Abstracts with Programs, v. 19, p. 714.
- Jacobson, C.E., Dawson, M.R., and Postlethwaite, C.E., 1988, Structure, metamorphism and tectonic significance of the Pelona, Orocoopia and Rand Schists, southern California, in Ernst, W.G., ed., *Metamorphism and crustal evolution in the western United States: Rubey Volume 7: Englewood Cliffs, New Jersey*, Prentice-Hall, p. 976–997.
- Jacobson, C.E., Oyarzabal, F.R., and Haxel, G.B., 1996, Subduction and exhumation of the Pelona-Orocoopia-Rand schists, southern California: *Geology*, v. 24, p. 547–550.
- Jacobson, C.E., Barth, A.P., and Grove, M., 2000, Late Cretaceous protolith age and provenance of the Pelona and Orocoopia Schists, southern California: Implications for evolution of the Cordilleran margin: *Geology*, v. 28, p. 219–222.
- Jennings, C.W., compiler, 1967, Geologic map of California—Salton Sea sheet: California Division of Mines and Geology, scale 1:250 000.
- Johnston, I.M., 1961, Eocene foraminifera from the lower Maniobra Formation, Orocoopia Mountains, Riverside County, California [M.A. thesis]: Berkeley, University of California, 93 p.
- Karcz, I., 1972, Sedimentary structures formed by flash floods in southern Israel: *Sedimentary Geology*, v. 7, p. 161–182.
- Karpeta, W.P., 1993, Volcanism and sedimentation of a Late Archean rift: The Harbeesfontein basin, Transvaal, South Africa: *Basin Research*, v. 5, p. 1–19.
- Leeder, M.R., and Gawthorpe, R.L., 1987, Sedimentary models for extensional tilt-block/half-graben basins, in Coward, M.P., et al., eds., *Continental extensional tectonics: Geological Society [London] Special Publication 28*, p. 139–152.
- Legg, M.R., 1991, Developments in understanding the tectonic evolution of the California continental borderland, in Osborne, R.H., and Lidz, B.D., eds., *From shoreline to abyss: Contributions in marine geology in honor of Francis Parker Shepard: Society of Economic Paleontologists and Mineralogists Special Publication 46*, p. 291–312.
- Lowe, D.R., 1979, Sediment gravity flows: Their classification and problems of application to natural flows and deposits, in Doyle, L.J., and Pilkey, O.H., eds., *Geology of continental slopes: Society of Economic Paleontologists and Mineralogists Special Publication 27*, p. 75–82.
- Lowe, D.R., 1982, Sediment gravity flows: II. Depositional models with special reference to the deposits of high-density turbidity currents: *Journal of Sedimentary Petrology*, v. 52, p. 279–297.
- Lowell, J.D., 1995, Mechanics of basin inversion from worldwide examples, in Buchanan, J.G., and Buchanan, P.G., eds., *Basin inversion: Geological Society [London] Special Publication 88*, p. 39–58.
- Luyendyk, B.P., 1991, A model for Neogene crustal rotations, transension and transpression in southern California: Geological Society of America Bulletin, v. 103, p. 1528–1536.
- Luyendyk, B.P., Kamerling, M.J., and Terres, R.R., 1980, Geometric model for Neogene crustal rotations in southern California: Geological Society of America Bulletin, v. 91, p. 211–217.
- Luyendyk, B.P., Kamerling, M.J., Terres, R.R., and Hornafius, J.S., 1985, Simple shear of southern California during Neogene time suggested by paleomagnetic declinations: *Journal of Geophysical Research*, v. 90, no. B14, p. 12454–12466.
- Mancktelow, N., 1989, Stereoplot, v. 1.2, Stereographic software for the Macintosh system: Zurich, Switzerland, Eidgenössische Technische Hochschule.
- Matt, J.C., and Morton, D.M., 1993, Paleogeographic evolution of the San Andreas fault in southern California: A reconstruction based on a new cross-fault correlation, in Powell, R.E., et al., eds., *The San Andreas fault system: Displacement, palinspastic reconstruction and geologic evolution: Geological Society of America Memoir 178*, p. 107–160.
- McClay, K.R., 1995, The geometries and kinematics of inverted fault systems: A review of analogue model studies, in Buchanan, J.G., and Buchanan, P.G., eds., *Basin inversion: Geological Society [London] Special Publication 88*, p. 97–118.
- McKee, E.D., Crosby, E.J., and Berryhill, H.L., Jr., 1967, Flood deposits, Bijou Creek, Colorado, June 1965: *Journal of Sedimentary Petrology*, v. 37, p. 829–851.
- Miall, A.D., 1977, A review of the braided-river depositional environment: *Earth Science Reviews*, v. 13, p. 1–62.
- Morris, R.S., 1993, Tertiary basin structure revealed in seismic reflection profiles from Milpitas Wash, southeastern California, in Sherrod, D.R., and Nielsen, J.E., eds., *Tertiary stratigraphy of highly extended terranes, California, Arizona, and Nevada: U.S. Geological Survey Bulletin 2053*, p. 217–234.
- Nemec, W., and Steel, R.J., 1984, Alluvial and coastal conglomerates: Their significant features and some comments on gravelly mass-flow deposits, in Koster, E.H., and Steel, R.J., eds., *Sedimentology of gravels and conglomerates: Canadian Society of Petroleum Geologists Memoir 10*, p. 1–34.
- Nicholson, C., Sorlien, C.C., Atwater, T., Crowell, J.C., and Luyendyk, B.P., 1994, Microplate capture, rotation of the Western Transverse Ranges, and initiation of the San Andreas transform as a low-angle fault system: *Geology*, v. 22, p. 491–495.
- Nilsen, T.H., 1982, Alluvial fan deposits, in Scholle, P.A., and Spearing, D., eds., *Sandstone depositional environments: American Association of Petroleum Geologists Memoir 31*, p. 49–86.
- Nilsen, T.H., and Sylvester, A.G., 1995, Strike-slip basins, in Busby, C.J., and Ingersoll, R.V., eds., *Tectonics of sedimentary basins: Oxford, UK, Blackwell*, p. 425–457.
- Nur, A., Ron, H., and Beroza, G., 1993, Landers-Mojave earthquake line: A new fault system? *GSA Today*, v. 3, p. 256–258.
- O'Day, P.A., and Simms, J.D., 1986, Sandstone composition and paleogeography of the Temblor Formation, central California: Evidence for early to middle Miocene right-lateral displacement on the San Andreas fault system: Geological Society of America Abstracts with Programs, v. 18, p. 165.
- Oyarzabal, F.R., Jacobson, C.E., and Haxel, G.B., 1997, Extensional reactivation of the Chocolate Mountains subduction thrust in the Gavilan Hills of southeastern California: *Tectonics*, v. 16, p. 650–661.
- Picard, M.D., and High, L.R., 1973, Sedimentary structures of ephemeral streams: Developments in sedimentology No. 17: Amsterdam, Elsevier, 223 p.
- Postlethwaite, C.E., and Jacobson, C.E., 1987, Early history and reactivation of the Rand thrust, southern California: *Journal of Structural Geology*, v. 9, p. 195–206.
- Powell, R.E., 1981, Geology of the crystalline basement complex, Eastern Transverse Ranges, southern California [Ph.D. thesis]: Pasadena, California, California Institute of Technology, 441 p.
- Powell, R.E., 1993, Balanced palinspastic reconstruction of pre-late Cenozoic paleogeography, southern California; geologic and kinematic constraints on evolution of the San Andreas fault system, in Powell, R.E., et al., eds., *The San Andreas fault system: Displacement, palinspastic reconstruction and geologic evolution: Geological Society of America Memoir 178*, p. 1–106.
- Powell, R.E., and Weldon, R.J., II, 1992, Evolution of the San Andreas fault: *Annual Review of Earth and Planetary Sciences*, v. 20, p. 431–468.
- Pridmore, C.L., and Frost, E.G., 1992, Detachment faults, California's extended past: *California Geology*, v. 45, p. 3–17.
- Ramsay, J.G., 1967, *Folding and fracturing of rocks: New York*, McGraw Hill, 568 p.
- Richard, S.M., 1988, Late Oligocene–early Miocene volcanism, faulting, and sedimentation in west-central California: *American Association of Petroleum Geologists Bulletin*, v. 72, p. 370–398.
- Richard, S.M., 1993, Palinspastic restoration of southeastern California and southwestern Arizona for the middle Miocene: *Tectonics*, v. 12, p. 830–854.
- Richard, S.M., and Haxel, G.B., 1991, Progressive exhumation of the Orocoopia and Pelona schists along a composite normal fault system, southeastern California and southwestern Arizona: *Geological Society of America Abstracts with Programs*, v. 23, no. 2, p. 92.
- Robinson, K.L., and Frost, E.G., 1989, Orocoopia Mountains detachment system; progressive ductile to brittle development of a tilted crustal slab during regional extension: *Geological Society of America Abstracts with Programs*, v. 21, no. 5, p. 135.
- Robinson, K.L., and Frost, E.G., 1991, Tertiary extension and basin development in southern California: The temporal similarity, style of deformation and crustal geometry in the Orocoopia Mountains and the San Joaquin Hills: *Geological Society of America Abstracts with Programs*, v. 23, no. 5, p. A132–A133.
- Robinson, K.L., and Frost, E.G., 1996, Orocoopia Mountains detachment system: Progressive development of a tilted crustal slab and a half-graben sedimentary basin during regional extension, in Abbott, P.L., and Cooper, J.D., eds., *Field conference guidebook and volume for the American Association of Petroleum Geologists, Annual Convention, San Diego, California: Bakersfield, Pacific Section American Association of Petroleum Geologists Guidebook 73*, p. 277–284.
- Ron, H., and Nur, A., 1996, Vertical axis rotations in the Mojave: Evidence from the Independence dike swarm: *Geology*, v. 24, p. 973–976.
- Ron, H., and Nur, A., 1997, Vertical axis rotations in the Mojave: Evidence from the Independence dike swarm: Comment and reply: *Geology*, v. 25, p. 1052.
- Rosendahl, B.R., 1987, Architecture of continental rifts with special reference to East Africa: *Annual Review of Earth and Planetary Sciences*, v. 15, p. 445–503.
- Ross, T.M., Luyendyk, B.P., and Haston, R.B., 1989, Paleomagnetic evidence for Neogene clockwise rotations in the central Mojave Desert: *Geology*, v. 17, p. 470–473.
- Schultejan, P.A., 1984, The Yaqui Ridge antiform and detachment fault: Mid-Cenozoic extensional terrane west of the San Andreas: *Tectonics*, v. 3, p. 677–691.
- Sheffels, B., and McNutt, M., 1986, Role of subsurface loads and regional compensation in the isostatic balance of the Transverse Ranges, California: *Journal of Geophysical Research*, v. 91, p. 6419–6431.

- Shen-Tu, B., and Holt, W.E., 1999, Deformation kinematics in the western United States determined from Quaternary fault slip rates and recent geodetic data: *Journal of Geophysical Research*, v. 104, p. 28927–28955.
- Shen-Tu, B., Holt, W.E., and Haines, A.J., 1998, The contemporary kinematics of the western United States determined from earthquake moment tensors, VLBI and GPS observations: *Journal of Geophysical Research*, v. 103, p. 18087–18117.
- Sherrod, D.R., and Nielsen, J.E., eds., 1993, Tertiary stratigraphy of highly extended terranes, California, Arizona, and Nevada: U.S. Geological Survey Bulletin 2053, 250 p.
- Sherrod, D.R., and Tosdal, R.M., 1991, Geologic setting and Tertiary structural evolution of southwestern Arizona and southeastern California: *Journal of Geophysical Research*, v. 96, p. 12407–12423.
- Silver, L.T., 1971, Problems of crystalline rocks of the Transverse Ranges: *Geological Society of America Abstracts with Programs*, v. 3, p. 193–194.
- Simpson, C., 1986, Microstructural evidence for northeastward movement on the Vincent–Orocopia–Chocolate Mountain thrust system: *Geological Society of America Abstracts with Programs*, v. 18, p. 186.
- Simpson, C., 1990, Microstructural evidence for northeastward movement on the Chocolate Mountains fault zone, southeastern California: *Journal of Geophysical Research*, v. 95, p. 529–537.
- Simpson, R.W., Howard, K.A., and Haxel, G.B., 1991, Introduction to special section on the California-Arizona crustal transect: CACTIS, Part 3: *Journal of Geophysical Research*, v. 96, p. 12257–12258.
- Spittler, T.E., 1974, Volcanic petrology and stratigraphy of non-marine strata, Orocopia Mountains; their bearing on Neogene slip on the San Andreas fault, southern California [M.S. thesis]: Riverside, University of California, 115 p.
- Spittler, T.E., and Arthur, M.A., 1982, The lower Miocene Diligencia Formation of the Orocopia Mountains, southern California: Stratigraphy, petrology, sedimentology, and structure, in Ingersoll, R.V., and Woodburne, M.O., eds., Cenozoic nonmarine deposits of California and Arizona: Los Angeles, Pacific Section, Society of Economic Paleontologists and Mineralogists, p. 83–99.
- Squires, R.L., and Advocate, D.M., 1982, Sedimentary facies of the nonmarine lower Miocene Diligencia Formation, Canyon Spring area, Orocopia Mountains, southern California, in Ingersoll, R.V., and Woodburne, M.O., eds., Cenozoic nonmarine deposits of California and Arizona: Los Angeles, Pacific Section, Society of Economic Paleontologists and Mineralogists, p. 101–106.
- Stanley, R.G., 1985, Middle Tertiary sedimentation and tectonics of the La Honda basin, central California: U.S. Geological Survey Open-File Report 85–596, 263 p.
- Stanley, R.G., 1987, New estimates of displacement along the San Andreas fault in central California based on paleobathymetry and paleogeography: *Geology*, v. 15, p. 171–174.
- Stein, R.S., King, G.C.P., and Lin, J., 1992, Change in failure stress on the southern San Andreas fault system caused by the 1992 $M=7.4$ Landers earthquake: *Science*, v. 258, p. 1328–1332.
- Stewart, J.H., 1998, Regional characteristics, tilt domains, and extensional history of the late Cenozoic Basin and Range province, western North America, in Faults, J.E., and Stewart, J.H., eds., Accommodation zones and transfer zones: The regional segmentation of the Basin and Range province: *Geological Society of America Special Paper* 323, p. 47–74.
- Swirydzuk, K., Wilkinson, B.H., and Smith, J.R., 1979, The Pliocene Glenns Ferry oolite: Lake margin carbonate deposition in the southwestern Snake River Plain: *Journal of Sedimentary Petrology*, v. 49, p. 995–1104.
- Sylvester, A.G., 1988, Strike-slip faults: *Geological Society of America Bulletin*, v. 100, p. 1666–1703.
- Sylvester, A.G., and Smith, R.R., 1975, Structure section across the San Andreas fault zone, Mecca Hills, in Crowl, J.C., ed., San Andreas fault in southern California: A guide to the San Andreas fault from Mexico to Carrizo Plain: California Division of Mines and Geology Special Report 118, p. 111–118.
- Sylvester, A.G., and Smith, R.R., 1976, Tectonic transpression and basement-controlled deformation in San Andreas fault zone, Salton Trough, California: *American Association of Petroleum Geologists Bulletin*, v. 60, p. 2081–2102.
- Tedford, R.H., Skinner, M.F., Fields, R.W., Rensberger, J.M., Whistler, D.P., Galusha, T., Taylor, B.E., MacDonald, J.R., and Webb, S.D., 1987, Faunal succession and biochronology of the Arikarean through Hemphillian intervals (late Oligocene through earliest Pliocene epochs) in North America, in Woodburne, M.O., ed., Cenozoic mammals of North America: Los Angeles, University of California Press, p. 153–210.
- Tennyson, M.E., 1989, Pre-transform early Miocene extension in western California: *Geology*, v. 17, p. 792–796.
- Terres, R.R., 1984, Paleomagnetism and tectonics of the central and Eastern Transverse Ranges, southern California [Ph.D. thesis]: Santa Barbara, University of California, 323 p.
- Terres, R.R., and Luyendyk, B.P., 1985, Neogene tectonic rotation of the San Gabriel region, California, suggested by paleomagnetic vectors: *Journal of Geophysical Research*, v. 90, p. 12467–12484.
- Terres, R.R., Luyendyk, B.P., and Marshall, M., 1981, Major clockwise rotation of the Diligencia basin of southeastern California [abs.]: *Eos (Transactions, American Geophysical Union)*, v. 62, p. 855.
- Tosdal, R.M., Haxel, G.B., and Dillon, J.T., 1986, Evidence for, and tectonic implications of, northeastward movement on the Chocolate Mountains thrust: *Geological Society of America Abstracts with Programs*, v. 18, p. 193.
- Tunbridge, I.P., 1981, Sandy high-energy flood sedimentation—Some criteria for recognition, with an example from the Devonian of S.W. England: *Sedimentary Geology*, v. 28, p. 79–95.
- Wallace, R.D., 1982, Evaluation of possible detachment faulting west of the San Andreas fault, southern Santa Rosa Mountains, California [M.S. thesis]: San Diego, California State University, 77 p.
- Weldon, R.J., II, Meisling, K.E., and Alexander, J., 1993, A speculative history of the San Andreas fault in the Central Transverse Ranges, California, in Powell, R.E., ed., The San Andreas fault system: Displacement, palinspastic reconstruction and geologic evolution: *Geological Society of America Memoir* 178, p. 161–198.
- Wells, R.E., and Hillhouse, J.W., 1989, Paleomagnetism and tectonic rotation of the lower Miocene Peach Springs Tuff, Colorado Plateau, Arizona to Barstow, California: *Geological Society of America Bulletin*, v. 101, p. 846–863.
- Wilcox, R.E., Harding, T.P., and Seeley, D.R., 1973, Basic wrench tectonics: *American Association of Petroleum Geologists*, v. 57, p. 74–96.
- Wolfe, J.A., 1986, Tertiary plant megafossils and paleoclimates of the northern hemisphere, in Gastaldo, R.A., ed., Land plants: Notes from a short course: Knoxville, The Paleontological Society, p. 182–196.
- Woodburne, M.O., and Whistler, D.P., 1973, An early Miocene oreodont (Merchyinae, Mammalia) from the Orocopia Mountains, southern California: *Journal of Paleontology*, v. 47, p. 908–912.
- Wust, S., 1986, Regional correlation of extension directions in the Cordilleran metamorphic core complexes: *Geology*, v. 14, p. 828–830.
- Zoback, M.L., Zoback, M.D., Adams, J., Bell, S., Suter, M., Suarez, G., Jacob, K., Estabrook, C., and Magee, M., 1991, Stress map of North America: *Geological Society of America, Continent-Scale Map* 005, 4 sheets, scale 1 : 5 000 000.

MANUSCRIPT RECEIVED BY THE SOCIETY JUNE 23, 1997
 REVISED MANUSCRIPT RECEIVED JANUARY 18, 2000
 MANUSCRIPT ACCEPTED MARCH 20, 2000

Printed in the USA